

1 **GROUND TEMPERATURES, LANDFORMS AND PROCESSES IN AN ATLANTIC**
2 **MOUNTAIN. CANTABRIAN RANGE (NORTHERN SPAIN)**

3
4 Pisabarro, A.¹, Pellitero, R.², Serrano, E.¹, Gómez-Lende, M.¹, González-Trueba,
5 J.J.³

6
7 ¹Dept. Geografía. Universidad de Valladolid, Spain.

8 ² School of Geosciences. St. Mary's, Elphinstone Road. University of Aberdeen, AB24 3UF. United
9 Kingdom.

10 ³ Dept. Geografía. CIESE-Comillas, Fundación Comillas – Universidad de Cantabria, Spain.
11
12

13 **Abstract**

14 Ground temperatures determine significant geomorphological processes in wet and
15 temperate mountain with a narrow high mountain belt. 25 temperature data
16 loggers were buried at a shallow depth in different locations and altitudes and at
17 specifically cold locations at two massifs in the Cantabrian Range (North Spain),
18 Picos de Europa and Fuentes Carrionas. This paper analyses the ground thermal
19 regime and associated parameters (e.g. freeze index, duration and depth of freeze,
20 freeze and thaw cycles) and correlates them with active geomorphological
21 processes and landforms. The thermal regime varies in accordance to the
22 topoclimatic conditions, and it was possible to determinate annual phases in
23 function of snow cover behaviour. Main active processes and landforms stop their
24 activity with a large snow cover which thermally protects the ground and in
25 consequence, avoids the freeze and thaw cycles. During this period, the records
26 allow to asseverate the evidence of seasonal freeze grounds in several locations.
27 Permafrost was not discover on the ground at any of the thermometers except one
28 located at the vicinity of a relict ice patch. With the help of geomorphological maps
29 1:25.000 and previous works, we got to establish the relation between
30 geomorphological processes, landforms, snow cover and ground thermal regime.

31
32 **Key words:** Ground Thermal Regime, Temperate High Mountain, Snow cover,
33 Geomorphology.
34
35

1. Introduction

The Cantabrian Range is characterized by a narrow periglacial belt, occupying the highest portions of the mountain, always above 1900 m.a.s.l.

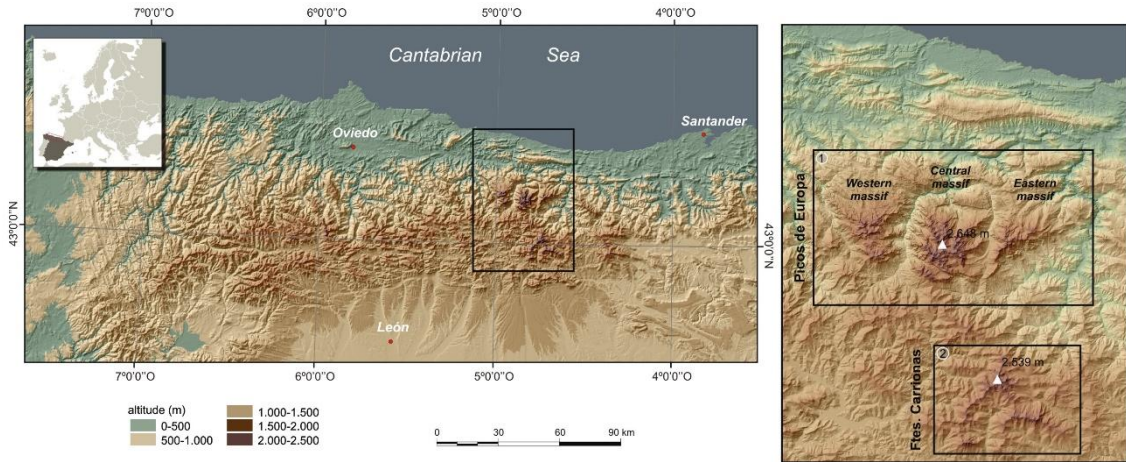


Figure 1. Location of Cantabrian Range and the massifs studied.

The most representative elements of the cryosphere in the Cantabrian Range are mainly the snow cover, seasonal freeze ground, and, to a lesser extent, ice patches, ice caves and sporadic permafrost, which are only located only in very specific locations. The snow cover is a key element in the high mountain, extending its effects to lower altitudes, with a socioeconomic value and a natural risk for settlements in the valleys. The snow cover is a cryosphere transversal component that influences on ground and surface waters, the physical soil compartment, the biogeochemical flows and the ecosystem dynamic (De Walle and Rango, 2008; Adam et al., 2009), determines partially the periglacial processes and affects the ground temperature and runoff regimes (Zhang, 2005; López-Moreno et al., 2009, García-Ruíz et al. 2011).

Permafrost is defined as the ground that remains at or below 0°C for at least two consecutive years (French, 2007; Dobinski, 2011). Particularly, mountain permafrost is characterised by discontinuities and instabilities derived from slope aspects, solar radiation and snow cover variability (Harris et al. 2009; Gruber and Haeberli, 2009). In Picos de Europa (PE) permafrost has been identified at sheltered local climates, always close to the ice patches (González-Trueba, 2007; Serrano et al. 2011). Ice caves are considerate as an endokarst permafrost environment, with permanent ice mass (Gómez-Lende et al. 2014; Gómez-Lende, 2015). Finally, the seasonal frozen ground (SFG) is key to understand the geomorphological processes in the Cantabrian high mountain.

65

66 The aim of the study is differentiate between the processes related to ice, snow or
67 gravity, as well as to determine the ground thermal regime in different locations,
68 establishing the magnitude and duration of the cold wave penetration by means of
69 the Freeze Index (FI), frozen ground season, number and timing of freeze-thaw
70 cycles (F/Tc). These measurements are related to the processes and landforms
71 developed in the Cantabrian high mountain, in order to detect the effectiveness of
72 current processes associated with ice on the ground.

73

74 This paper deals with the highest massifs in the Cantabrian Range, where the active
75 periglacial landforms (e.g. frost mounds, debris flows, terracettes and solifluction
76 lobes) are most common. In both cases the depth of the cryogenic processes
77 remains unknown. PE has the highest altitudes in the Cantabrian Range, up to 2648
78 m.a.s.l. It comprises an area of 150 sq. km. Lithology is mostly calcareous, and
79 limestones thickness reach about 2000 meters. Relief is very abrupt and ruled by
80 the development of the locally called "jous", which are deep glaciokarstic
81 depressions between ice-moulded horns (Fig.1). The seasonal snow cover
82 generates superficial and underground karstic processes, which are mostly directed
83 by layers stratification and faulting. On relict glacial and periglacial deposits, snow
84 melt and frost-heave play a role in the general deposit erosion. This also happens
85 to bedrock over 1800 m.a.s.l. There is also relict glacial ice in several sheltered
86 locations. Fuentes Carrionas (FC) is the second highest massif in the Cantabrian
87 Range. It is structurally more complex than PE, and hosts a more varied lithology.
88 Bedrock is generally siliceous, although there are some limestone outcrops too. It
89 highest area is located at a central syncline with conglomerates, slates and the
90 largest granite outcrop of the entire range.

91

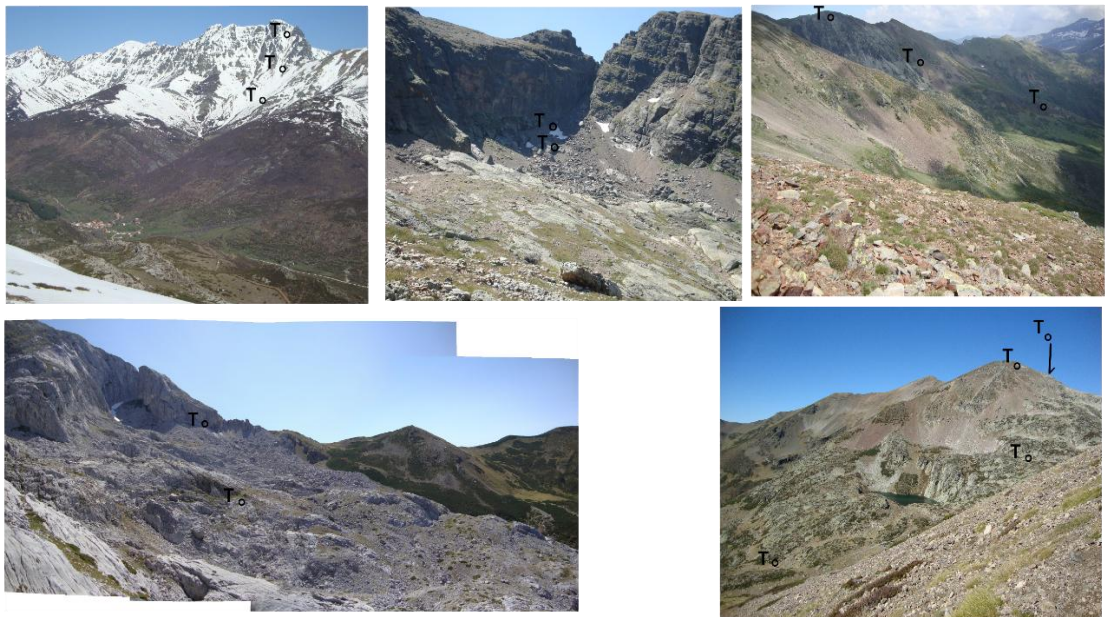
92 Both massifs get the highest amount of precipitations between November and May,
93 most of it as snow (González-Trueba y Serrano, 2010). Precipitations reach 1900
94 mm/year in PE (Fig.5), thanks to its proximity to the Cantabrian Sea, whereas in FC
95 they are about 1000 mm/year due to the shadow effect from the PE. Snow
96 precipitation is highly variable depending on the year. First snow of the season
97 usually falls in early autumn, but summer snow is possible, and dry years can delay
98 snowfall up to March during dry and cold winters.

99



100
 101
 102
 103
 104
 105

Figure 2. Locations of the thermometers in Picos de Europa massif. Left to right and up to down: Jou Traslambrión, Peña Vieja, Áлива, Jou Negro, Lloroza, Fuente De.



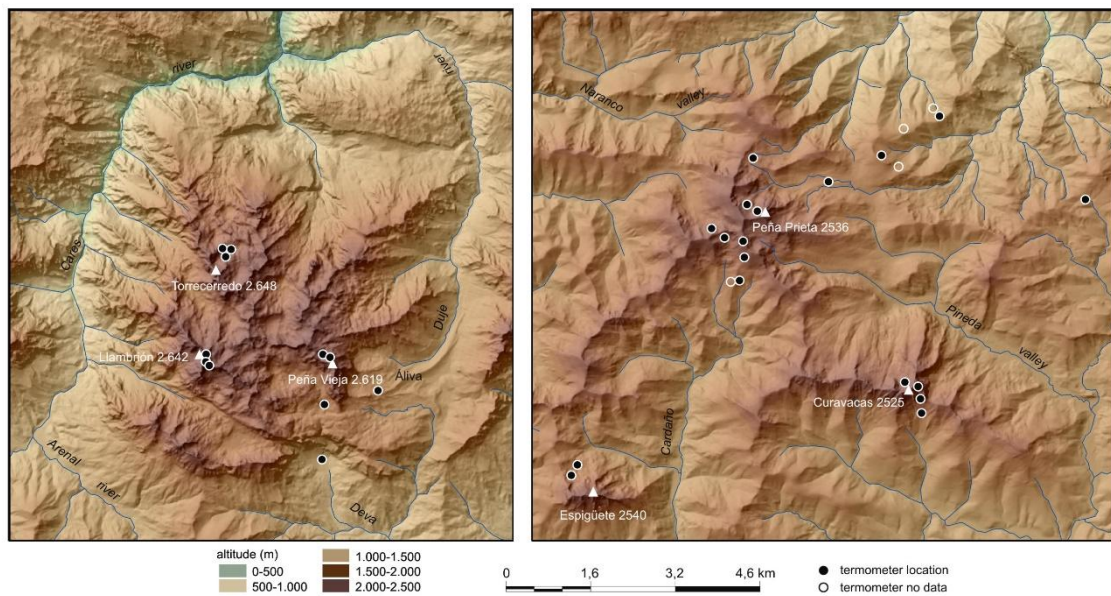
106
 107
 108
 109
 110

Figure 3. Locations of the thermometers in Fuentes Carrionas massif. Left to right and up to down: South face of Curavacas peak, N cirque of Curavacas peak, W faced slope in Tio Celestino peak, N face of Espiguete peak and E face of Lomas peak.

2. Materials and methods

111
112
113
114
115
116
117
118
119

Ground thermal regimes were obtained by thermal micro sensors I-bottom UTL - Geotest AG (Universal Temperature Logger) data-logger with centesimal accuracy and 0.05°C error level. They were buried between 0.1 and 0.2 meters depth, following Delaloye (2004) methodology. These thermometers allow monitoring ground temperatures between 4 and 6 times a day for an entire year. Thermometer locations are visible in Figures 2, 3, 4 and Table 1. The data was taken between 2004 and 2007 in PE and between 2009 and 2012 in FC.



120
121
122
123
124
125
126
127
128
129
130
131
132
133
134
135

Figure 4. Left, massif of Picos de Europa and right, massif of Fuentes Carrionas.

Main data treatment consisted in obtaining representative statistical parameters, tendencies, cycles and temporal behaviours; with an emphasis on the freeze index (FI) (Fengqing and Yanwei, 2011). FI has been useful to compare ground seasonal freeze depths and its magnitude (SFG) (French, 2007).

Periglacial landforms were mapped at a 1/25000 scale in PE (González-Trueba, 2007; González-Trueba y Serrano, 2010; González-Trueba et al., 2012; Serrano and González-Trueba, 2004) and 1/12.000 in FC (Pellitero, 2014), allowing the inventory of landforms related to periglacial processes.

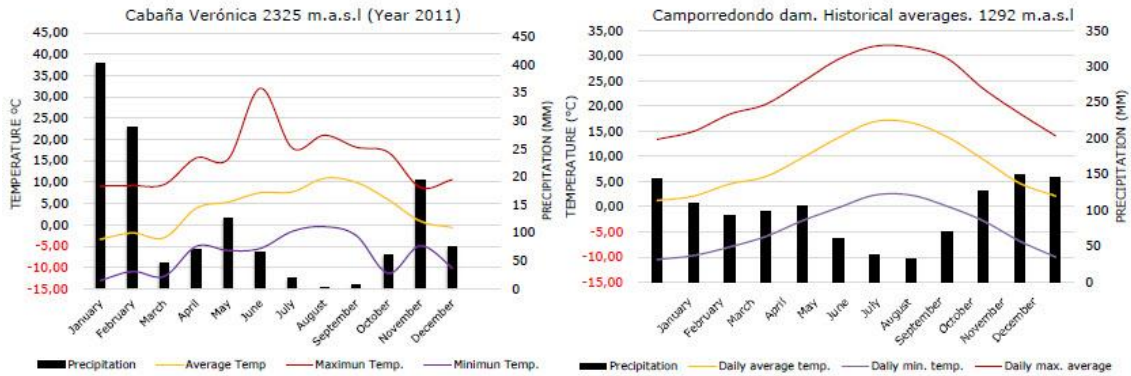
The meteorological station analysis has allowed us to estimate the average annual temperatures, the number of days below 0°C and -2°C, FI and F/Tc after 3 high mountain weather stations in PE and one station in valley at FC.

136
137
138
139
140
141
142

3. Results

3.1. Air thermal regimes

In PE, the AAMT is 3.6°C at 2325 m.a.s.l., the atmospheric high freeze index is high and snowpack depths are around 2 m of thickness. The snow cover is stable between December/January to May/June. Atmospheric minimum temperature can get below -10°C between October and March according to 2011 values.



143
144
145

Figure 5. Air temperature and precipitation approximately in PE (left) and FC (right).

146 There are not high mountain weather stations in Fuentes Carrionas, but we can find
147 several ones in the nearby valleys. Camporredondo de Alba (1295 m.a.s.l.) has the
148 longest lasting record among them, with more than 80 years of daily records of
149 precipitation and temperature. Here, AAMT is 8° C and the minimum daily
150 temperature is below -5°C between November and April and below 0° all months
151 except summer.

3.2. Ground thermal values

3.2.1. Freeze magnitude

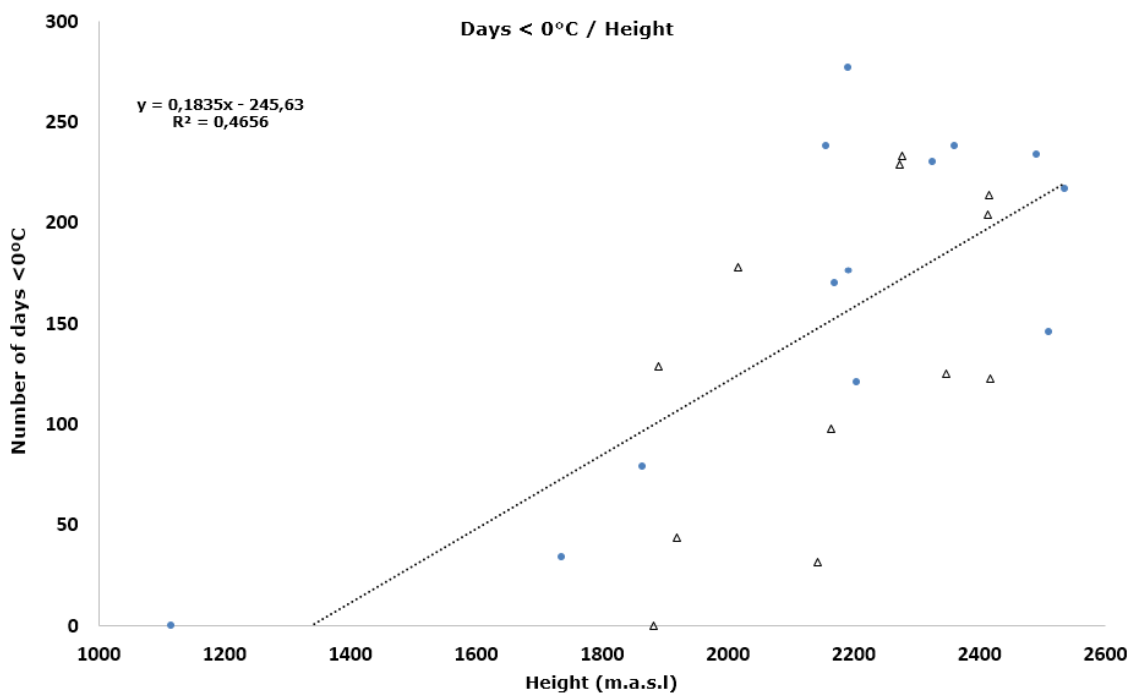
154 The number of days with temperatures below 0°C exceeds half of the year over
155 2100 m.a.s.l. At some particularly high locations the ground is kept frozen over
156 75% of the year. These areas also record sustained temperatures below -2°C. The -
157 2°C threshold is considered the highest winter temperature to consider the
158 existence of sporadic permafrost (Haeberli, 1973; French, 2007). There are six
159 locations where the -2°C limit is continuously exceeded, mainly in Lomas (FC) over
160 2400 m.a.s.l. and Jou Negro (PE) over 2150 m.a.s.l. However, the low
161 temperatures are not kept long enough to consider the existence of permafrost
162 (Fig. 7). The thermometers located at the moraine by the ice-patch in Jou Negro
163 (Fig. 2) are the ones with highest freeze index, which is coherent with the existence

164 of frost mounds at the site. This could show the influence of the nearby ice body
165 and maybe other buried frozen bodies within the moraine (González-Trueba, 2007).
166 Below 2000 m.a.s.l. the FI is low in both massifs (between 55 and 0) and under
167 100 below 2100 meters. In general, FI is highly dependent on the snow cover,
168 which keeps the soil around 0°C thanks to the zero curtain effect. This situation is
169 especially marked in FC, where thermometers were placed at different orientations
170 in order to highlight the snow accumulation changes. Here, over 2100 meters,
171 where the snow mantle is stable, the FI is close to 0, especially at the N and E
172 slope, but on the W and S orientations, or at very steep slopes where the snow
173 mantle is not stable, the FI exceeds 100. Therefore, the most exposed soils are the
174 ones where the periglacial processes are more active. Frozen ground days are
175 conversely maximum where the snow mantle is most stable, with values over 260
176 days near semi-permanent snow-patches.

177

178 Given the similarities between the studied massifs, the thermometer altitude and
179 days below zero degrees have been correlated. There is a linear correlation
180 between altitudes of both massifs and number of days $T_g < 0^\circ\text{C}$ with p-value < 0.05
181 and $r^2 = 0.4592$. This is interpreted a statistically significant correlation, but other
182 factors, as the mentioned orientation, snow cover and situation near relict ice
183 patches, must be also considered.

184



185

186

Figure 6. Correlation between thermometers in FC (triangles) and PE (points).

Name Massif	Height	Asp	Lat °	Long °	Deposit	Bedrock	Year	Days < 0°C	%	Days < -2°C	%	FI	F/Tc	T°C (Phase3)	SFG	Frozen ground depth (m) ^[1]	Conductivity (J*°day) (Eppelbaum et al. 2014)
Espigüete	FC	1889	N 42,9517	4,7984	Terra rossa in doline	Limestone	08/09-11/12	129	36,2	1	0,3	30	6	0 to 0,5	Unlikely	0,29	2,05*10 ⁵
Espigüete	FC	2016	N 42,9491	4,8011	Debris on active scree	Limestone	2010/12	178	50,0	3	0,8	67	14	-3 to 0,5	Likely	0,39	2,05*10 ⁵
Lomas	FC	1918	E 43,0032	4,7397	Soil on till sheet	Turbidite	2010/12	44	12,4	0	0,0	39	6	-0,5 to 0,5	Likely	0,28	1,44*10 ⁵
Lomas	FC	2163	W 43,0097	4,7381	Soil on scree	Turbidite	2009/12	98	27,5	0	0,0	33	36	-1 to 0	Likely	0,27	1,44*10 ⁵
Lomas	FC	2417	W 43,0150	4,7380	Blockfield	Granite	2009/11	123	34,5	60	16,8	273	54	-7 to 0,5	Yes	0,72	2,32*10 ⁵
Lomas	FC	2169	E 43,0132	4,7440	Soil on till sheet	Granite	2010/12	170	47,7	0	0,0	67	24	-0,5 to -0,5	Likely	0,40	2,32*10 ⁵
Lomas	FC	2412	E 43,0156	4,7502	Soil on scree	Granite	2010/12	204	57,3	0	0,0	69	4	-0,5 to 0	Likely	0,41	2,32*10 ⁵
Lomas	FC	2415	N 43,0158	4,7506	Solifluction lobe	Sandstone	2010/12	214	60,1	11	3,1	109	8	-3 to 0,5	Yes	0,48	2,16*10 ⁵
Curavacas	FC	1882	S 42,9683	4,6698	Soil on scree	Conglomerate	2010/12	0	0,0	0	0,0	0	0	-	Unlikely	0,00	4,32*10 ⁵
Curavacas	FC	2143	S 42,9729	4,6711	Soil on scree	Conglomerate	2010/12	32	9,0	0	0,0	0	6	0 to 0,5	Unlikely	0,00	4,32*10 ⁵
Curavacas	FC	2346	S 42,9756	4,6723	Soil over bedrock	Conglomerate	2010/12	125	35,1	14	3,9	77	4	-2,5 to 0	Yes	0,55	4,32*10 ⁵
Curavacas (2)	FC	2272	N 42,9759	4,6786	Active scree	Conglomerate	2010/12	229	64,3	0	0,0	0	2	0 to 0,5	Unlikely	0,00	4,32*10 ⁵
Curavacas (1)	FC	2277	N 42,9756	4,6786	Active scree	Conglomerate	2010/12	233	65,4	0	0,0	0	4	0	Likely	0,00	4,32*10 ⁵
Llambrión	PE	2535	N 43,1736	4,8528	Till in rock bar	Limestone	2005/07	217	60,9	0	0,0	85	15	-0,5 to 0	Likely	0,42	2,05*10 ⁵
Traslambrión	PE	2490	N 43,1748	4,8541	Till in rock bar	Limestone	2005/07	234	65,7	2	0,6	219	8	-1,5 to -0,3	Yes	0,62	2,05*10 ⁵
Traslambrión	PE	2360	N 43,1792	4,8533	Top debris cone	Limestone	2005/07	238	66,8	0	0,0	59	3	-0,5 to 0	Likely	0,37	2,05*10 ⁵
Jou Negro	PE	2205	N 43,2027	4,8499	Debris slope	Limestone	2005/07	121	34,0	2	0,6	113	10	-1,5 to -0,5	Yes	0,47	2,05*10 ⁵
Jou Negro	PE	2155	N 43,2022	4,8521	Till in moraine	Limestone	2005/07	238	66,8	65	18,2	235	18	-1,1 to -0,1	Yes	0,64	2,05*10 ⁵
Jou Negro	PE	2190	N 43,2019	4,8525	Till -patterned ground	Limestone	2005/07	176	49,4	63	17,7	461	40	-8,5 to 0	Yes	0,77	1,64*10 ⁵
Jou Negro(Ta)	PE	2190	N 43,2019	4,8525	Till -patterned ground	Limestone	2005/07	277	77,8	1	0,3	138	36	-2,5 to -0,1	Yes	0,37	1,64*10 ⁵
Peña Vieja	PE	2510	W 43,1747	4,8106	Debris slope	Limestone	2003/04	146	41,0	17	4,8	96	9	-1 to 0	Likely	0,41	1,64*10 ⁵
Peña Vieja	PE	2325	W 43,1753	4,8122	Small sinkhole	Limestone	2003/05	230	64,6	0	0,0	20	15	-0,2 to 0,2	Likely	0,26	2,05*10 ⁵
Lloroza	PE	1865	S 43,1597	4,8120	Moraine	Limestone	2005/07	79	22,2	2	0,6	55	8	-0,7 to 0,5	Likely	0,33	1,64*10 ⁵
Áliva	PE	1735	E 43,1944	4,7714	Soil with debris	Shales	2005/07	34	9,5	0	0,0	3	6	0 to 0,5	Likely	0,15	1,44*10 ⁵
Fuente Dé	PE	1115	S 43,1492	4,8098	Debris cone	Limestone	2005/07	0	0,0	0	0,0	0	0	-	Unlikely	0,00	2,05*10 ⁵

[1] Washburn (1979): $f(m) = \sqrt{\frac{2 * K * FI}{C_L}} + d$; K (Conductivity J*°day); CL (Latent Heat 3,34*108J *m-3); FI (Freeze Index °day); d (depth of the register 0,1)

188 Table 1. Main parameters of the thermometers in Picos de Europa and Fuentes Carrionas.

189

190 Frozen ground depth was not measured in this project, but it can be calculated
 191 from the shallow-buried thermometer temperatures using the Washburn (1979)
 192 approach, taking into account that the used constants were calculated in laboratory
 193 conditions. The highest freeze depth was calculated for Jou Negro (PE) with 0.77 m.
 194 and Lomas (FC) with 0.72 m. The higher conductivity of the soil material in Lomas
 195 permits a higher potential for frost penetration in the ground regardless a lower FI.
 196 Anyway, these values entail that there is a considerable amount of soil susceptible
 197 to be mobilised during the thaw season. Not surprisingly, they coincide with the
 198 development of gelifluction lobes in Lomas (whose thickness is around 0.5 meters,
 199 see Fig. 11), which corroborates the effect of seasonal frost in the landform
 200 creation processes.

201

202 3.2.2. Freeze-thaw cycles (F/Tc)

203 The entire area presents F/Tc which are highly variable and dependant on the snow
 204 cover. F/Tc are more frequent on steep slopes, crest, wind-exposed areas and
 205 overhangs, where the snow cover is not stable. Sheltered situations reduce F/Tc
 206 to less than 18 cycles/year. F/Tc are generally higher in PE, especially in autumn and
 207 even summer (between 5 and 33 cycles in summer and autumn), whereas the F/Tc
 208 in winter and spring are similar in both massifs.

209

Picos de Europa	Alt.	Jan	Feb	Mar	Apr	May	Jun	Jul	Aug	Sept	Oct	Nov	Dec	Total	Year
Llambrión	2.535							1		1	2	2	9	15	2006
Peña Vieja	2.510					5						3	1	9	10/2003- 10/2004
Jou Traslambrión	2.490							1			1	6		8	2006
Jou Traslambrión	2.360							1	2					3	2006
Peña Vieja	2.325	13	1					1						15	2004
Jou Negro	2.205					5						3	2	10	2006
Jou Negro (Superficie)	2.190							1	2	5	8	14	4	34	11/2005-11/2006
Jou Negro	2.190	4							4	4	10	14	4	40	11/2005-11/2006
Jou Negro	2.155				4	4						6	4	18	2006
Lloroza	1.865			7									1	8	2006
Áliva	1.720	1	1	3	1									6	2005
Fuente Dé	1.115													0	2006
SubTotal		18	2	10	5	14	0	5	8	10	21	48	25		
Fuentes Carrionas	Alt.	Jan	Feb	Mar	Apr	May	Jun	Jul	Aug	Sept	Oct	Nov	Dec	Total	Year
Espiguete	1.889						1							1	2009/10
Espiguete	2.016				1						4	4		9	2010/11
Lomas E	1.918	1	1	1									1	4	2010/11
Lomas E	2.169				9	3						5	1	18	2010/11
Lomas E	2.412						1				1			2	2010/11
Lomas W	2.163	7	1	1									9	18	2010/11
Lomas W	2.417	9	13	8								3	11	44	2010/11
Lomas N	2.415					1					1	3		5	2010/11
Curavacas S	1.882													0	2010/11
Curavacas S	2.143		2	1										3	2010/11
Curavacas S	2.346				1								4	5	2010/11
Curavacas N low	2.272						1				1			2	2010/11
Curavacas N high	2.277						1				1			2	2010/11
Subtotal		17	17	11	11	4	4	0	0	0	8	15	26		
TOTAL		35	19	21	16	18	4	5	8	10	29	63	51		

210

211

212

Table 2. Monthly distribution of F/Tc in PE and FC.

213 The highest amount of F/Tc in both areas happens in autumn, when the snow
214 mantle is thin and brief. In spring/summer there are few cycles, between 1 and 5
215 over 2000 m.a.s.l., especially where the snow mantle can keep up to the late spring
216 or early summer. Here, snowmelt coincides with the existence of already high
217 atmospheric temperatures, which implies a higher thermal stress a soil that very
218 quickly passes from a zero-curtain winter effect, to summer high temperatures (see
219 Fig. 7 Jou Negro or Peña Vieja). The few summer cycles correspond to night
220 irradiation frost in clear summer nights at the highest elevations of PE, possibly
221 with the influence of nearby ice-patches.

222

223 **3.2.3. Ground thermal regimes: the climate at the soils**

224

225 The analysis of the ground daily temperatures reveals at least four thermal phases,
226 whose duration is variable depending on the topoclimatic peculiarities. Some of
227 these theoretical phases can be subdivided given specific thermal situations (Figs. 7
228 and 8).

229

230 The **high temperatures phase (1)** usually lasts from May or June until the
231 beginning of the autumn in early October. During this season the ground is in
232 contact with atmosphere and temperature is over 0°C. It. There is a strong
233 variability between days and nights when frost is possible. The difference between
234 consecutive daily temperatures is also highly variable, so it can reach up to 10°C.

235

236 **Transition Summer-Winter (2).** During this season, which is usually short and
237 not clearly defined in all cases, happening between October and early December,
238 temperatures get or even descend the 0°C. There is a great ground thermal
239 instability, which is originated by the first seasonal snowfall and the sudden
240 temperature drop over 2000 m.a.s.l. Snow mantle is settled in favourable aspects
241 (E and N, see Fig. 8), provoked by precipitations and lower temperatures carried by
242 Atlantic depressions and fronts. Nevertheless, the snow mantle is still ephemeral in
243 exposed areas, where the soil still gets the atmospheric influence, so some F/Tc
244 happen here, and the temperature oscillations gradually become colder. It is also
245 possible that sudden temperature increment, caused by the irruption of stable
246 tropical air, melts most of the snow (see November 2011 in Fig. 8). Only N and E
247 faces over 2150 m. escape the general snowmelt situation, mainly because many of
248 them remain in the shadow during this season.

249

250 **Isothermal equilibrium (3).** The onset of phase 3 is marked by a uniform 0°C,
251 due to the snow curtain effect. Its duration in Picos de Europa (Fig.7) varies
252 between 3 and 9 months depending on the altitude, with large differences between
253 years depending on the snow mantle thickness. In 2006 the cold wave was larger in
254 general but Jou Traslambrión and Jou Negro (2490 and 2205 m a.s.l.) had their
255 lowest temperatures in 2007, probably due to the snow instability or because of
256 inner thermal fluxes within the vicinity of buried ice. There are not frozen grounds
257 below 1800 meters in PE. In FC the ground thermal regime is much differentiated
258 depending on the orientation and altitude. N and E faced areas, where snow
259 accumulates (over 2000 m.a.s.l. in the glacial cirques and elsewhere over 2150
260 m.a.s.l.) and its mantle is stable between October and May-June, the F/Tc are
261 reduced to the autumn thermal freeze below the snow mantle and the melt in late
262 spring. The spring season melt saturates the surface at enables solifluction. At the
263 W/S faces the snow mantle is more unstable due to enhanced solar radiation and
264 wind blow-out.

265

266 As an example, thermometers at the S face show very distinctive behaviour
267 depending on the height. At 1900 m. on the S face there are not F/Tc and the snow
268 cover is not sufficient to create the curtain effect. At 2150 m. there are F/Tc but
269 temperatures in winter are near the 0°C, which show the curtain effect. Finally, the
270 thermometer installed over 2400 meters (Fig. 8) shows a strong freeze, with a Tg
271 <-7 °C on a snow disappearance situation in January 2011. These events imply a
272 deep freeze and therefore enhanced gelifluction and frost shattering.

273

274 **Snowmelt (4). This is a sudden episode in which the thermal transfer from**
275 **the atmosphere (which is often several degrees over 0°C)** attains the
276 ground. In N faced cirques, as Jou Negro, Traslambrión (PE) or Curavacas (FC) this
277 can happen at the onset of summer, during late June, so there is a sharp increase
278 to the Tg in accordance with the Ta. Temperature rises between 10°C and 20°C
279 during a single day, which prevents new F/Tc in summer. Finally, late snowfall can
280 lay a spring snow mantle which installs the curtain effect again for several days,
281 which enables new late F/Tc. This happened in May 2010 at the W face of Pico
282 Lomas.

283

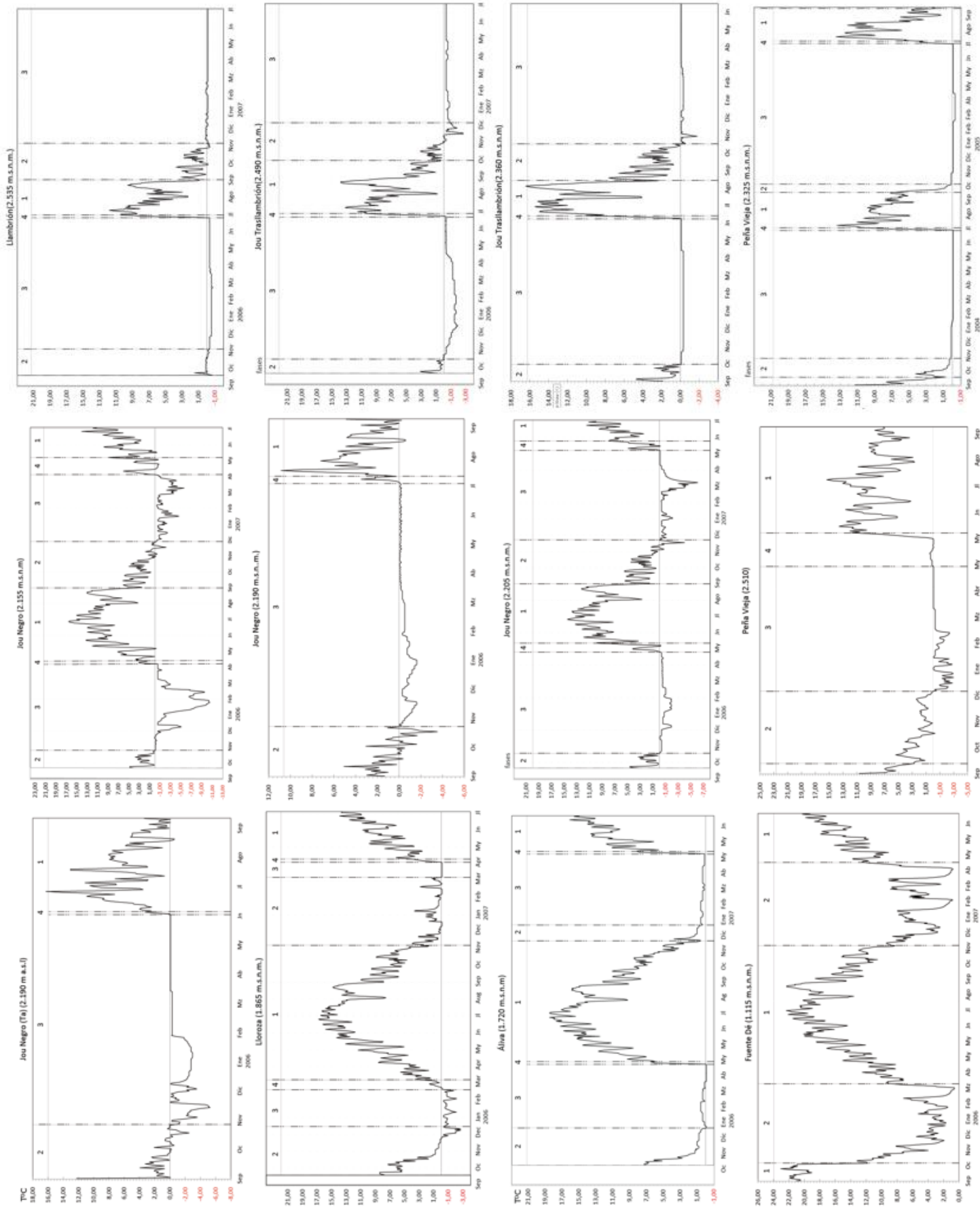


Figure 7. Ground thermal regimes of Picos de Europa

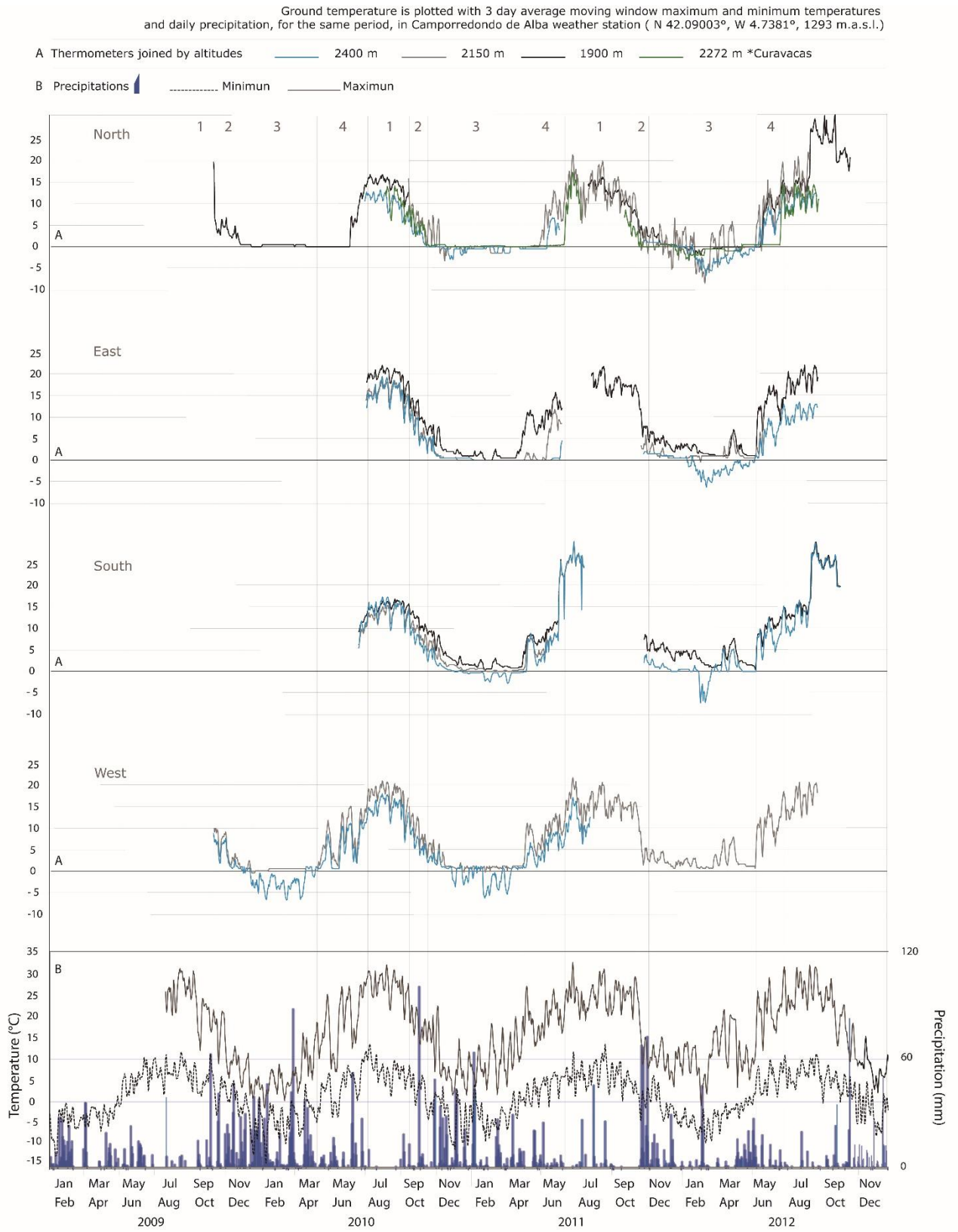


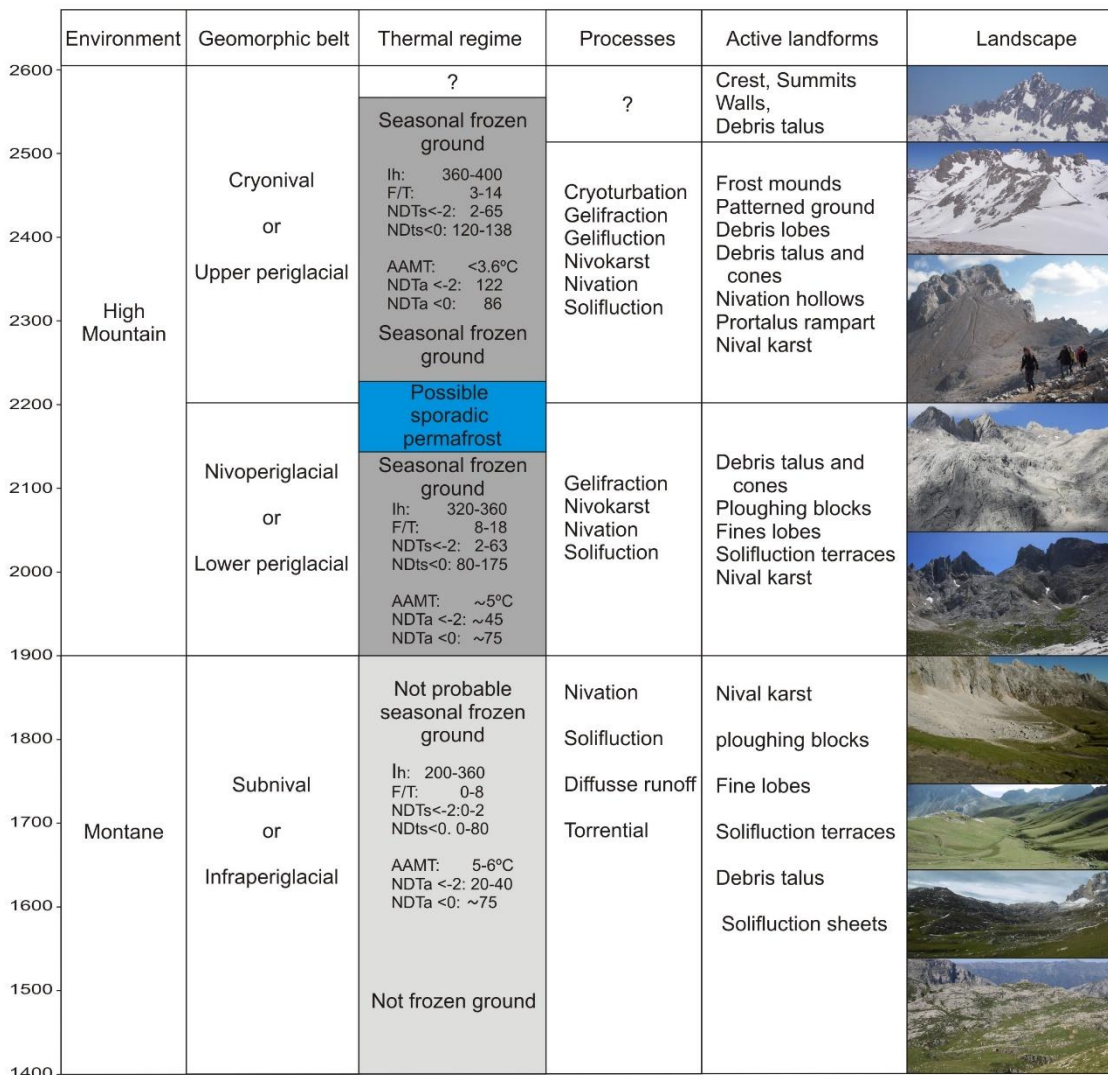
Figure 8. Ground thermal regimes of Fuentes Carrionas

289 **3.3. Landforms and processes**

290

291 The ground thermal regime in different altitudes shows several altitudinal steps.
 292 Depending on the altitudinal belt, the processes and landforms change (Figs. 9 and
 293 10). In Fuentes Carrionas SFG only appears at 1900 m.a.s.l. on the N face,
 294 whereas on the S face there are SFG over 2100. In Picos de Europa the SFG area is
 295 between 1900 m.a.s.l. to the top of data records (2535 m.a.s.l.). The distribution of
 296 the slope landforms in PE are characterized by processes of low intensity processes,
 297 except debris flow and snow avalanches. Landforms are linked to the gravity,
 298 freeze-thaw cycles, thermal cracking, creeping, solifluction and water saturation by
 299 rain and snow melt, often with close interrelationship with vegetation. Therefore, it
 300 is possible differentiate the altitudinal distribution of landforms.

301






302

303

304

Figure 9. Environments, thermal regime, processes and active landforms in PE.

	Environment	Geomorphic belt	Thermal regime	Processes	Active landforms	Landscape
2550	High mountain (alpine)	Cryonival	Seasonal frozen ground FI: 0-379 F/T: 2-58 NDTs <= -2°C: 0-92 NDTs <= 0°C: 117-244 AAMT: 3.5°C <i>Sporadic permafrost?</i>	Gelifraction Gelifluction Debris flow Rockfall Nivation Avalanches	Blockfields Stone-banked gelifluction lobes Protalus lobe? Walls Debris talus and cones Terracetes	
2500						
2450						
2400						
2350						
2300	Mid-mountain (montane)	Nivo-periglacial	Seasonal frozen ground FI: 0-151 F/T: 6-39 NDTs <= -2°C: 0-40 NDTs <= 0°C: 0-151 AAMT: 5.2°C	Nivation Solifluction Nival abrasion Avalanches	Debris talus and cones Turf-banked solifluction lobes Terracetes Nivation hollows Nival abrasion surfaces Snow-push moraines Ploughing boulders	
2250						
2200						
2150						
2100						
2050		Infraperiglacial	Seasonal frost only on N face FI: 0-39 F/T: 0-6 NDTs <= -2°C: 0-1 NDTs <= 0°C: 0-129 AAMT: 6.3°C	Runoff Torrential erosion Solifluction (N face)	Nival terracetes Ravines	
2000						
1950						
1900						
1850						
1800						
1750						
1700						

306

307

308

Figure 10. Environments, thermal regime, processes and active landforms in FC.

309

310 The **debris talus and cones** are one of the fastest sediment transfer in both
311 massifs.

312 They develop at an altitudinal range between 1800 m.a.s.l. and the peaks, although
313 in some exceptional occasions they develop as low as 1200 m.a.s.l. Their exact
314 location is very much directed by tectonics for the lowest ones, which are usually
315 located under fault and thrust scarps (Serrano y González-Trueba, 2004; González-
316 Trueba, 2007; González-Trueba y Serrano, 2010; González-Trueba et al. 2012;
317 Serrano et al. 2014). Over 2000 m.a.s.l. talus locate preferentially on N faces, and
318 they are fed by frost shattered clasts, debris flows and avalanches (Serrano and
319 González-Trueba, 2004, Serrano et al. 2014). The vertical development of these
320 landforms is quite varied, between 100 and 900 meters.

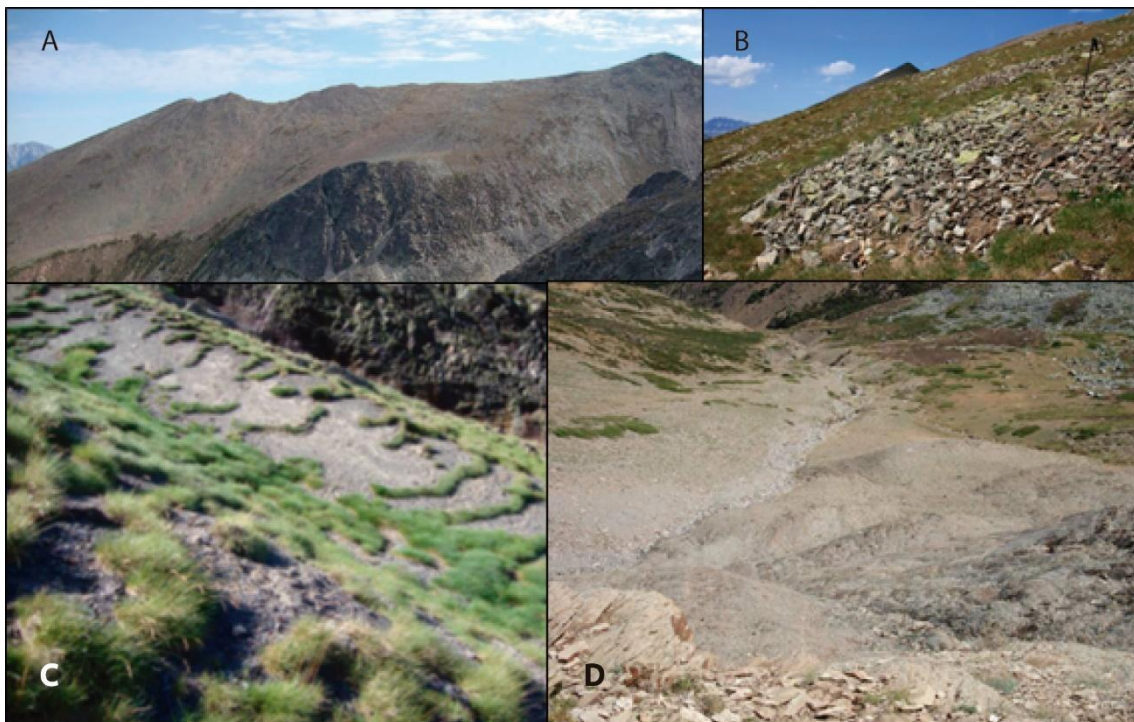
321

322 **The snow patches** are snow accumulations that melt between June and August,
323 and they can even endure the summer. Due to their specific thermal regime, water
324 saturation and slow ground creep, they form a complete array of singular
325 landforms. **Nivation hollows** are created by snow creep and snow-melt runoff, in
326 a context where persistent snow mantle also prevents plant colonization to happen.
327 They are located usually on glaciokarstic depressions or glacial tarns. We can also
328 find at the foot of patches **protalus ramparts**, originated by the slide of material
329 along the snow-patch and its accumulation at the foot. Nivation hollows and
330 protalus rampart have been mapped in PE between 1900 and 2400 m.a.s.l.

331 (González-Trueba 2007), although active landforms of this type are located over
332 2100 m.a.s.l. only on shadowed areas, being very active over 2400 m.a.s.l. In FC
333 these landforms are found over 1900 m.a.s.l. and on slopes $\sim 20^\circ$ of inclination,
334 also on N faces. Here some snow-push moraines, whose formation is originated due
335 to the frontal push of an unstable snow mantle (Kirkbride 2015). Associated to
336 these snow-push moraines there are also nival stone pavements and snow polished
337 bedrock, with associated striae and partly detached material (Fig. 11). These
338 landforms show a snow mantle basal drag on the bedrock.

339 **The debris lobes and stone banked solifluction lobes** are coarse grained
340 regolith masses that flow down. Their size is <1 m deep, ~ 4 o 5 long and ~ 2 m
341 wide, and they usually appear clustered in groups. In FC they are located mainly at
342 the W face of Tres Provincias Peak over 2300 m.a.s.l. on a $\sim 35^\circ$ slope. Here, there
343 is not a wall to provide material to the regolith, and the snow cover is never too
344 thick due to wind-blow of snow, so frost can penetrate deep in the ground (table 3).
345 Similar landforms can be found at the W, S and N slopes in Peña Prieta, over 2300
346 m.a.s.l. In PE these landforms can be found in Peña Vieja, over 2400 m.a.s.l.,
347 where displacements between 1.3 and 1.6 cm a^{-1} have been measured (Brosche,
348 1994) and in Jou Negro on till at 2240 m.a.s.l. (González-Trueba, 2007; Serrano et
349 al. 2011).

350



351
352 Figure 11. A) The W face of Tres Provincias peak, where the gelifluction lobes have
353 developed. B) Stone banked solifluction lobe. The lobe front shows fresh material at its front,
354 with not liquen-colonized clasts over fine-grained material and roots pulled downslope. C)
355 Nival melt solifluction terraces versus right periglacial solifluction terraces. Scarce vegetation

356 and a sufficient regolith is a must for their formation. Both terraces are formed on slate
357 lithology. D) Snow abraded surface and snow-push moraine at a cirque around 2000 m.a.s.l.
358 in FC

359

360 **Landforms linked to solifluction:** Fine grained, water saturated regolith is prone
361 to solifluction, which is also conditioned by the snow cover, the ground thermal
362 regime and the absence of vegetation (Brosche, 1978, 1994; González-Trueba,
363 2007). In PE solifluction processes have been measured to a range between 2.1
364 and 18.8 mm a^{-1} (Brosche, 1994). The **solifluction terraces** can be defined as
365 decimetric steps on slopes where their front is turf-banked (usually *Festuca* gender
366 turf), whereas the flat back is often vegetation free. Their vertical development is
367 around 20 cm., step longitude is usually around a meter and the lateral
368 development can attain several meters. Some terracettes are conversely related to
369 long lasting snow patches, which inhibit the vegetation to grow and provoke
370 solifluction on the snow melt season. These terracettes are longer and steeper than
371 those formed by several F/Tc (Fig. 11). In PE they sit on slopes between 15° and
372 40° steep, on fine grained superficial formations, such as moraines, colluvium or
373 debris talus, over 1500 m.a.s.l. In FC they are most ubiquitous periglacial landform
374 over 1950 m.a.s.l. where the lithology allows the formation of a surface regolith
375 with enough fine material (Fig. 11).

376 **Ploughing boulders** exist on slopes where large blocks move faster than the fine
377 matrix, always in a context of water availability and fine grained regolith. This
378 landform is scarce both in PE or FC, and usually it is linked to a slate or schist
379 bedrock above 1700 m. Measured displacements are very low, between 8 y 14 mm
380 a^{-1} (measured with DGPS between 2008 y 2014 in Áliva área, in Picos de Europa -
381 Sanjosé et al. 2016).

382 **Fine banked lobes** are metric to decametric solifluction lobes associated to a 30 –
383 40 cm. deep fine matrix regolith, also on shales, schist, till or sandstone. It is
384 located on $20\text{-}25^\circ$ slopes at an altitudinal range between 1500-1800 in PE and over
385 1900 m. in FC. The clayey regolith prevents water percolation, and once it is water
386 saturated, especially at the end of the spring season, it starts to flow downslope.
387 DGPS measurements in Áliva (PE.) between 2008 and 2014 show an average
388 annual displacement lower than 2 cms. yr^{-1} (Sanjosé et al. 2016). These landforms
389 are located at the transition between the highest portion of the mid-mountain belt
390 and the high mountain, in a pasturage landscape just over the treeline.

391 **Patterned ground:** Circles and stripes are located in plain areas with a fine
392 grained regolith, mainly on karstic depressions or on debris and till formation.
393 Stripes sizes are between 2-3 m in length and circles are between 40 and 150 cm
394 wide. They are always located above 2200 m. Active patterned ground has been

395 found PE at 2400 m in Peña Vieja, and semi-active ones at 2100 m (Brosche, 1994;
396 González-Trueba, 2007; Serrano and González-Trueba, 2011; Serrano et al. 2011).
397 In F.C some relict patterned grounds can be found too.

398 **Frost mounds** are the rarest periglacial landform in the Cantabrian Range. They
399 can only be found in the debris generated by a slide of the Little Ice Age moraine
400 on the Jou Negro relict ice-patch at 2200 meters in PE. These frost mounds have
401 been preserved during at least the last twenty years, and they are located on a
402 deposit where an ice core has been found beneath (González-Trueba, 2007;
403 González-Trueba et al, 2012; Serrano et al. 2011). They have been attributed to
404 the melt water flow on the ice patch and segregation ice growth on the supra-ice
405 debris, therefore they are not related to atmospheric conditions.

406

407 **4. Discussion**

408 Correlation between altitude and Tg is not strong. The described annual thermal
409 phases do not happen uniformly as a function of altitude, due to topoclimatic
410 factors such as solar radiation, snow redistribution and the existence of buried ice
411 bodies (Pisabarro et al. 2015). Nevertheless, nivation effect is present on the
412 ground thermal regime at any height over 2200 m.a.s.l. mostly restricting the F/Tc
413 by the zero curtain effect at the base of the snow mantle. This determines
414 geomorphological processes in the high mountain belt of the Cantabrian Range. As
415 a morphological agent, snow is responsible for the nival karst, snow accumulation
416 landforms at the proximity of snow patches and solifluction, in PE as low as 1400
417 m.a.s.l. Solifluction sheets, long-shaped terracettes and lobes are a consequence of
418 nival fusion and the subsequent water saturation of the regolith. Protalus rampart,
419 stone pavements and nivation hollows are conversely generated by material
420 dragging and accumulation at the foot of snow-patches.

421 Below 1900 m.a.s.l. the number of F/Tc is much reduced, because of high
422 temperatures and the snow mantle protection during winter; moreover, none of the
423 thermometers registered temperatures below -2°C. Nevertheless, in Áliva (PE,
424 1700 m.a.s.l.), solifluction on slopes is active or has been active recently.
425 Solifluction lobes and ploughing boulders, always genetically associated to laminar
426 solifluction (Ballantyne, 2001, Berthling et al., 2001) are found here. Solifluction
427 lobes depend on an array of climatic, hydrologic, geologic and topographic factors
428 (e.g. slope, land cover, soil moisture, snow mantle depth and duration or soil
429 thermal regime) (Matsuoka, 2001; Oliva et al. 2009, Oliva and Gómez-Ortíz, 2011).
430 In any case, they are associated to some extent with a frozen ground (French,
431 2007). In Áliva, the thermal record points to an absence of F/Tc. We offer two
432 interpretations for these landforms: either they are inherited, given their

433 displacement is $14 \text{ mm} \cdot \text{yr}^{-1}$ for the ploughing boulders and $5 \text{ mm} \cdot \text{yr}^{-1}$ for the
434 lobes, or originated by spring snowmelt in an water saturated environment. The
435 fine material abundance in the regolith, and human-induced deforestation and
436 overgrazing might play their role in this process.

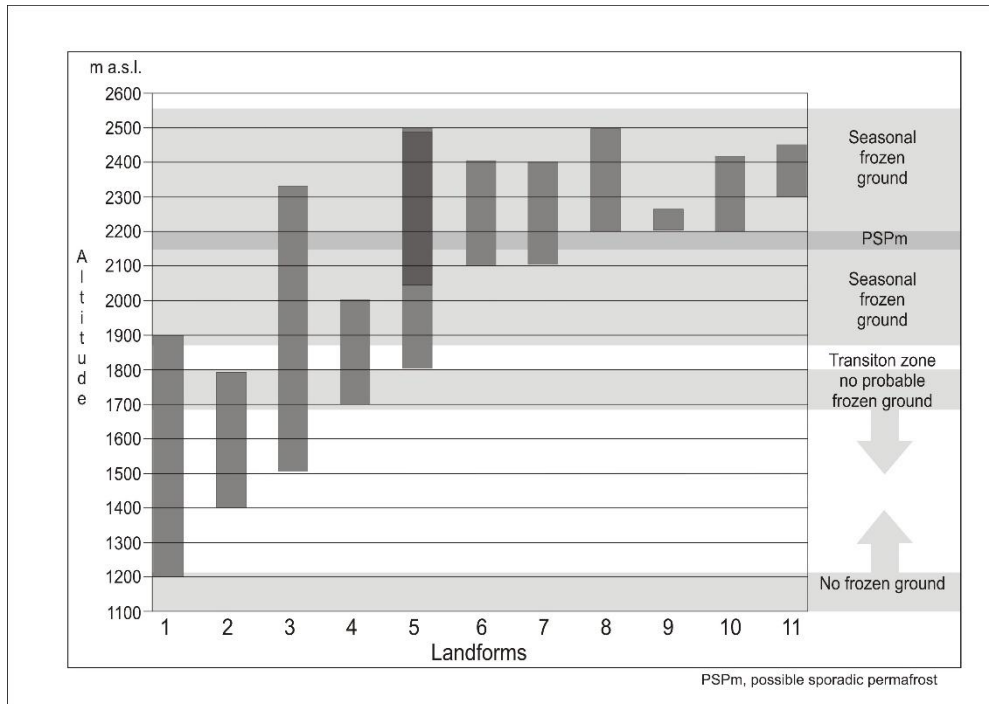
437

438 Above 1900 m.a.s.l. the thermal environment is defined by a strong disparity
439 between T_g and T_a . The F/T_c at this height are moderate and the FI can reach 461
440 in PE and 360 in FC. The ground keeps below 0°C up to 3 months, with a month of
441 temperatures below -2°C in PE. In FC the inter-annual differences are large
442 depending on the snowfall and the atmospheric temperature regime. The existence
443 of SFG can be associated to the existence of solifluction lobes in slopes and debris
444 cones, ploughing boulders and turf-banked solifluction lobes.

445 Screens and debris cones show a distinctive pattern depending on their altitude,
446 orientation and previous tectonic shattering of the rock. An intense previous rock
447 preparation enhances the thermally driven processes on the walls, such as frost or
448 thermal shattering. Ice effectiveness increases at the highest portions of screes and
449 debris cones.

450 The ground thermal data shows a highly variable snow mantle between 2008 and
451 2014, lasting between 2 months in 2013 and 7 in 2013 (table 5, Fig. 5), which
452 involves in turn a high thermal regime variability, with snow melt and runoff during
453 winter. South oriented slopes do not have active periglacial landforms below 2100
454 m.a.s.l. W oriented slopes combine a lower solar radiation and the snow blow-out,
455 so winter atmospheric frost is more intense, able to penetrate deeper in the
456 regolith, and F/T_c are also more abundant. Here, terracettes, blockfields and
457 gelifluction lobes are most extensively developed. N oriented slopes usually
458 maintain a thick snow mantle, which protects it from thermal oscillations. Here we
459 find most of the snow-patches and their associated landforms.

460 Over 2200 meters the FI is between 360-400, getting more than 430 at around
461 2500 m.a.s.l., and the soil keeps four months below 0°C , one of them below -2°C .
462 A FI >360 has been considered a SFG indicator (Fraunfeld et al. 2007); this value is
463 surpassed at the 2200 m.a.s.l., so the SFG is assured. AAMT is here moderately
464 cold (2°C) with an AAMT $<0^\circ\text{C}$ only over 2500 m.a.s.l. At N and E slopes over
465 2200 m.a.s.l. the snow mantle prevents an intense frost except in exposed areas.
466 Nevertheless, out of protected areas frost penetration is deep, and we can find
467 blockfields and gelifluction lobes, as per example near Peña Prieta, the highest peak
468 in FC (Pellitero et al. 2013).



469

470

471 Figure 12. Altitudinal distribution of environment, ground ice, landforms and processes in the
 472 Picos de Europa.

473

474 There is a large inter-annual disparity in the ground thermal regime, which reflects
 475 the different atmospheric dynamics along the year. Wet winters, as in 2009/10,
 476 entail a lower thermal stress on the ground, because snow cover protects it through
 477 the curtain-effect. Dry years, as in 2010/11, conversely generate a higher thermal
 478 stress on the ground, with more F/Tc and deeper thermal oscillations. Grounds at
 479 the peak can suffer a total snow blow-out and therefore get a deep freeze.
 480 Permafrost on the regolith can be ruled out in FC and almost certainly in PE, except
 481 in the latter case from inherited ice-patches (Jou Negro, Trasllambrión, Palanca and
 482 Forcadona) and frozen caves, which can be considered an endokarst permafrost
 483 (Gómez-Lende, 2015). The seasonal frost action cannot be dismissed, and it was
 484 captured by Brown et al. 2014 in the world permafrost and frozen ground map.

485

486 5. Conclusions

487

488 The snow cover control is the main geomorphological factor for periglacial
 489 processes because the wave of cold is blocked. This, joined to another topoclimatic
 490 factors (aspect, radiation, slopes, convective movements, wind, and superficial
 491 deposits) are the key to characterize the ground thermal regime and a

492 geocological belt in a wet and temperate high mountain. In PE, limestone
493 lithology makes easy the irradiation of cold from ice bodies beneath and the
494 permafrost formation, but the general lack of soil and regolith inhibits the formation
495 of solifluction landforms. In Fuentes Carrionas, the more impermeable lithologies
496 (conglomerates, granites, sandstones and turbidites) and fine-grained superficial
497 deposits permits the formation of periglacial features, which are widespread over
498 2000 meters.

499

500 Both massifs have a correlation between days $<0^{\circ}$ C and their altitude. However
501 this correlation does not exist with days below -2° C. The buried and surface iced
502 bodies in PE is the cause for abnormal low temperatures in some selected locations.
503 In others, the snow cover prevents the ground temperatures to go lower than 0° C.
504 Therefore, there is not altitudinal gradient of ground minimal temperatures above
505 1700 – 1800 m.a.s.l. Topoclimatic factors explain both the minimum temperature
506 and the SFG. The maximum depth of SFG is close to 0.7 m, a magnitude order
507 similar to the vertical active periglacial landforms over 2100 m.a.s.l. like frost
508 mounds and gelifluction lobes. Such a SFG is achieved only on the mentioned ice-
509 patches in PE and on exposed (W face and unsheltered N locations) soils over 2400
510 m. in FC, where the minimum temperatures are also lowest and the snow cover is
511 not continuous or deep. The most active periglacial processes, associated to the
512 gelifluction and frost-heave, are also generated at these locations. Between 2400
513 and 1900 meters the slope dynamics is ruled by the combination of freeze/thaw
514 cycles (most common at the W aspects) and snowmelt (on E and N aspects). Below
515 1900 m.a.s.l. the ice influence on the ground is negligible. Solifluction landforms at
516 this height have no relation with freeze/thaw cycles, but with spring snowmelt.

517

518 November and December are the months with most F/Tc, with 41% of the total
519 annual cycles. This is due to the arrival of cold arctic air without the protection of a
520 snow mantle on the ground, so the cycles are generalized at all orientations. At this
521 point steep temperature gradients are also present, as well as daily thermal
522 amplitudes over 5° C. This is a moment for intensification of periglacial processes.
523 This behaviour can extend into the winter and even early spring on exceptionally
524 dry years, but gives way to the winter and spring regime, in which the snow cover
525 imposes a thermal equilibrium around 0° C with located values below -2° C and a
526 general SFG over 1900 m. (PE) and 2000 m. (FC). Spring snowmelt and defrost
527 reactivates periglacial and nival processes and affects to a shallow soil or regolith
528 layer between 0.3 and 0.7 m. depth.

529

530 Overall, the nival and periglacial geomorphological processes are exceptional in the
531 Cantabrian Range high mountain, and they are only located in climatically
532 favourable locations. In PE they are mostly related to relict ice masses, or inherited
533 from the colder Little Ice Age. In FC periglacial processes are active on exposed
534 slopes over 2000, whereas snow-related processes are predominant on the N and E
535 face, where freeze/thaw cycles are limited to spring snowmelt.
536

537 **Acknowledgements**

538 This research was supported by the Formación de Profesorado Universitario
539 FPU13/05837 (Ministerio de Educación Cultura y Deporte) program, by the OAPN
540 053/2010 (Organismo Autónomo Parques Nacionales, MAGRAMA) project, by the
541 I+D+I CGL2015-68144-R (Ministerio de Economía y Competitividad) project, by the
542 Leverhulme Trust International Network Grant IN-2012-140 and the RGS Dudley
543 Stamp Memorial Award.

544 **References**

- 545
- 546 Adam, J. C., Hamlet, A. F., Lettenmaier, D.P. 2009. Implications of global climate
547 change for snowmelt hydrology in the twenty-first century. *Hydrological
548 Processes* 23(7): 962-972. <http://dx.doi.org/10.1002/hyp.7201>.
- 549 Ballantyne, C.K. 2001. Measurement and theory of ploughing boulder movement.
550 *Permafrost and Periglacial Processes*, 12 (3): 267-288.
551 <http://dx.doi.org/10.1002/ppp.389>.
- 552 Berthling, I., Eiken, T., Ludvig, S. 2001. Frost heave and thaw consolidation of
553 ploughing boulders in a mid-alpine environment, Finse, Southern Norway.
554 *Permafrost and Periglacial Processes*, 12 (2): 165-177.
555 <http://dx.doi.org/10.1002/ppp.367>.
- 556 Brosche, K.U. 1978. Beiträge zum rezenten und vorzeitlichen periglazialen
557 Formenschatz auf der Iberischen Halbinsel. *Abhandlungen des Geographischen
558 Instituts, Sonderhefte, Band I. Selbstverlag des Geographischen Instituts der
559 Freien Universität Berlin.* 285 pp.
- 560 Brosche, K.U. 1994. Ergebnisse von Abtragungsmessungen an periglazialen
561 Solifluktionsschuttdecken in vier Hochgebirgen der Iberischen Halbinsel (Picos
562 de Europa, Peña Prieta, Sierra de Urbión und Sierra Nevada). *Eiszeitalter u.
563 Gegenwart*, 44, 28-55.
- 564 Brown, J., Ferrians, O., Heginbottom, J.A., Melkinov, E. 2014. Circum-Arctic Map of
565 Permafrost and Ground-Ice Conditions. [On Line]. Boulder, Colorado USA:

566 National Snow and Ice Data Center. Available in:
567 <<http://nsidc.org/data/ggd318>> [Access 03 March 2015].

568 Castañón, J.C., Frochoso, M. 1998. La alta montaña cantábrica: condiciones
569 térmicas y morfodinámicas en los Picos de Europa. En: Gómez Ortiz, A.,
570 Salvador Franch, F., Schulte, L., García Navarro A. (Eds.), Procesos biofísicos
571 actuales en medios fríos, 113-132, Publicaciones Universidad de Barcelona,
572 Barcelona.

573 De Walle, R. Y Rango A. 2008. Principles of snow hydrology. Cambridge University
574 Press, Cambridge. <http://dx.doi.org/10.1017/cbo9780511535673>.

575 Delaloye, R. 2004. Contribution à l'étude du pergélisol de montagne en zone
576 marginale. PhD thesis, Fac. Sciences, Univ. Fribourg, GeoFocus, 10.

577 Dobinski, W. 2011. Permafrost. *Earth-Science Reviews*, 108, 158–169.
578 <http://dx.doi.org/10.1016/j.earscirev.2011.06.007>.

579 Eppelbaum, L., Kutasov, I., Pilchin, A. 2014. Thermal Properties of Rocks and
580 Density of Fluids. In *Applied Geothermics*, Springer, 99-149.
581 http://dx.doi.org/10.1007/978-3-642-34023-9_2.

582 Fengqing, J., Yanwei, Z. 2011. Freezing and thawing index, in: Singh, V.P., Singh,
583 P., Haritashya, U.K. (Eds.). *Encyclopedia of snow, ice and glaciers*, Springer,
584 Netherlands, pp. 301-301. doi.org/10.1007/978-90-481-2642-2_16.

585 Frauenfeld, O.W., Zhang, T., McCreight, J.L. 2007. Northern hemisphere
586 freezing/thawing index variations over the twentieth century. *International*
587 *Journal of Climatology*, 27, 47–63. <http://dx.doi.org/10.1002/joc.1372>.

588 French, H.M. 2007. *The periglacial environment*. Wiley, pp. 478, Chichester, United
589 Kingdom. <http://dx.doi.org/10.1002/9781118684931>.

590 García-Ruiz J.M., López-Moreno, J.I. Serrano-Vicente S.M., Beguería, S. & Lasanta,
591 T. 2011. Mediterranean water resources in a global change scenario. *Earth*
592 *Science Reviews*, 105 (3-4), 121-139.
593 <http://dx.doi.org/10.1016/j.earscirev.2011.01.006>.

594 Gómez-Lende, M., 2015. Las cuevas heladas en Picos de Europa: clima, morfologías
595 y dinámicas, Tesis Doctoral. Universidad de Valladolid, Valladolid.

596 Gómez-Lende, M., Berenguer F., Serrano E. 2014. Morphology, ice types and
597 thermal regime in a high mountain ice cave. First studies applying terrestrial
598 laser scanner in the Peña Castil Ice Cave (Picos de Europa, Northern Spain).
599 *Geografía Física e Dinámica Cuaternaria* 37, 141-150.
600 <http://dx.doi.org/10.5038/1827-806x.43.1.4>.

601 González-Trueba, J.J. 2007. *Geomorfología del Macizo Central del Parque Nacional*
602 *de Picos de Europa*. OAPN-Ministerio de Medio Ambiente, Madrid.

603 González-Trueba, J.J., Serrano, E. 2010. Geomorfología del Macizo Oriental del
604 Parque Nacional de Picos de Europa. OAPN-Ministerio de Medio Ambiente,
605 Madrid.

606 González-Trueba, J.J.; Serrano, E.; González García, M. 2012. Geomorfología del
607 Macizo Occidental del Parque Nacional de Picos de Europa. OAPN – Ministerio
608 de Medio Ambiente, Madrid.

609 Gruber, S., Haeberli, W. 2009. Mountain permafrost, in. Margesin, R. (Ed.).
610 Permafrost Soils, Biology Series, pp 33– 44, Springer Verlag.
611 http://dx.doi.org/10.1007/978-3-540-69371-0_3.

612 Haeberli, W. 1973. Die Basis-Temperatur der winterlichen Schneedecke als
613 möglicher Indikator für die Verbreitung von Permafrost in den Alpen, Z.
614 Gletscherkd. Glazialgeol, 9, 221–227.

615 Kirkbride, M.P. 2015. A Snow-Push Mechanism for Ridge Formation in the
616 Cairngorm Mountains, Scotland, Scottish Geographical Journal. 132:1, 66-73.
617 <http://dx.doi.org/10.1080/14702541.2015.1068948>.

618 Harris, C., Arenson, L. U., Christiansen, H. H., Etzelmüller, B., Frauenfelder, R.,
619 Gruber, S. ... Vonder Mühl, D. 2009. Permafrost and climate in Europe:
620 Monitoring and modelling thermal, geomorphological and geotechnical
621 responses. Earth-Science Reviews. 92(3-4), 117–171.
622 [doi:10.1016/j.earscirev.2008.12.002](https://doi.org/10.1016/j.earscirev.2008.12.002).

623 López-Moreno, J.I., Goyette, S., Beniston, M. 2009. Impact of climate change on
624 snowpack in the Pyrenees: Horizontal spatial variability and vertical gradients
625 Journal of Hydrology. 374 (3-4), 384-396.
626 <http://dx.doi.org/10.1016/j.jhydrol.2009.06.049>.

627 Matsuoka, N. 2001. Solifluction rates, processes and landforms: a global review.
628 Earth Science Reviews 55, 107-134. [http://dx.doi.org/10.1016/s0012-](http://dx.doi.org/10.1016/s0012-8252(01)00057-5)
629 [8252\(01\)00057-5](http://dx.doi.org/10.1016/s0012-8252(01)00057-5).

630 May, B., Spötl, C., Wagenbach, D., Dublyansky, Y., Liebl, J. 2011. First
631 investigations of an ice core from Eisriesenwelt cave (Austria), The Cryosphere
632 5, 81-93. <http://dx.doi.org/10.5194/tc-5-81-2011>.

633 Oliva, M., Schulte, I., Gómez-Ortíz, A. 2009. Morphometry and Late Holocene
634 activity of solifluction landforms in the Sierra Nevada, Southern Spain.
635 Permafrost and Periglacial Processes, 20 (4), 369-382.
636 <http://dx.doi.org/10.1002/ppp.645>.

637 Oliva, M., Gómez-Ortíz, A. 2011. Factores que condicionan los procesos
638 periglaciares de vertiente actuales en Sierra Nevada. El caso de la soliflucción.
639 Nimbus 27-28: 137-158.

640 Pellitero, R. 2013. Geomorfología, paleoambiente cuaternario y geodiversidad en el
641 macizo de Fuentes Carrionas-Montaña Palentina. Tesis Doctoral. Departamento
642 de Geografía, Universidad de Valladolid, Valladolid.

643 Pellitero, R., 2014. Geomorphology and geomorphological landscapes of Fuentes
644 Carrionas. *J. Maps* 10, 313–323.
645 <http://dx.doi.org/10.1080/17445647.2013.867822>.

646 Pisabarro, A., Serrano, E. & González-Trueba, J.J. 2015. Régimen térmico de suelos
647 del Macizo Central de Picos de Europa (España). *Pirineos. Revista de Ecología
648 de Montaña*, 170, <http://dx.doi.org/10.3989/Pirineos.2015.170003>.

649 Sanjosé, J.J., Serrano, E., Gómez Lende, M. 2016. Análisis geomático de bloques
650 aradores y lóbulos en los puertos de Aliva (Picos de Europa, Cordillera
651 Cantábrica). *Polígonos*, 28, in press.

652 Serrano, E.; González-Trueba, J.J. 2004. Morfodinámica periglacial en el grupo
653 Peña Vieja (Macizo Central de los Picos de Europa – Cantabria). *Cuaternario y
654 Geomorfología* 18 (3-4):73-88.

655 Serrano, E.; González-Trueba, J.J.; Sanjosé, J.J.; Del Río, L.M. 2011. Ice
656 patch origin, evolution and dynamics in a temperate maritime high mountain:
657 the Jou Negro, Picos de Europa (NW Spain). *Geografiska Annaler*, 93, 2, 97-
658 70. <http://dx.doi.org/10.1111/j.1468-0459.2011.00006.x>.

659 Serrano, E.; González-Trueba, J.J., González-García, M. 2012. Mountain glaciation
660 and paleoclimate reconstruction in the Picos de Europa (Iberian Peninsula, SW
661 Europe). *Quaternary Research* 78, 303-314.
662 <http://dx.doi.org/10.1016/j.yqres.2012.05.016>.

663 Serrano, E., González-Trueba, J.J., Pellitero, R., González-García, M., Gómez-
664 Lende, M. 2013. Quaternary glacial evolution in the Central Cantabrian
665 Mountains (Northern Spain). *Geomorphology* 196, 65-82.
666 <http://dx.doi.org/10.1016/j.geomorph.2012.05.001>.

667 Serrano, E., Gómez-Lende, M., González-Amuchastegui, M.J., González-García, M.,
668 González-Trueba, J.J., Pellitero, R., Rico, I. 2014. Glacial chronology,
669 environmental changes and implications on the human occupation during the
670 upper pleistocene in the eastern Cantabrian Mountains. *Quaternary
671 International*, doi 10.1016/j.quaint. 2014.09.039.

672 Washburn, A.L. 1979. *Geocryology. A survey of periglacial processes and
673 environments*. Arnold, 406 pp., Londres.

674 Zhang, T. 2005. Influence of the seasonal snow cover on the ground thermal
675 regime: an overview. *Reviews of Geophysics*, 43, 1-23
676
677

Table1. Main parameters of the thermometers in Picos de Europa a
[Click here to download Table: Table 1.pdf](#)

Name Massif	Height	Asp	Lat °	Long °	Deposit	Bedrock	Year	Days < 0 °C	%	Days < -2 °C	%	FI	F/Tc	T °C (Phase3)	SFG	Frozen ground depth (m) ^[1]	Conductivity (J* °day) (Epelebaum et al. 2014)
Espigüete	FC	1889	N 42,9517	4,7984	Terra rossa in doline	Limestone	08/09-11/12	129	36,2	1	0,3	30	6	0 to 0,5	Unlikely	0,29	2,05*10 ⁵
Espigüete	FC	2016	N 42,9491	4,8011	Debris on active scree	Limestone	2010/12	178	50,0	3	0,8	67	14	-3 to 0,5	Likely	0,39	2,05*10 ⁵
Lomas	FC	1918	E 43,0032	4,7397	Soil on till sheet	Turbidite	2010/12	44	12,4	0	0,0	39	6	-0,5 to 0,5	Likely	0,28	1,44*10 ⁵
Lomas	FC	2163	W 43,0097	4,7381	Soil on scree	Turbidite	2009/12	98	27,5	0	0,0	33	36	-1 to 0	Likely	0,27	1,44*10 ⁵
Lomas	FC	2417	W 43,0150	4,7380	Blockfield	Granite	2009/11	123	34,5	60	16,8	273	54	-7 to 0,5	Yes	0,72	2,32*10 ⁵
Lomas	FC	2169	E 43,0132	4,7440	Soil on till sheet	Granite	2010/12	170	47,7	0	0,0	67	24	-0,5 to -0,5	Likely	0,40	2,32*10 ⁵
Lomas	FC	2412	E 43,0156	4,7502	Soil on scree	Granite	2010/12	204	57,3	0	0,0	69	4	-0,5 to 0	Likely	0,41	2,32*10 ⁵
Lomas	FC	2415	N 43,0158	4,7506	Solifluction lobe	Sandstone	2010/12	214	60,1	11	3,1	109	8	-3 to 0,5	Yes	0,48	2,16*10 ⁵
Curavacas	FC	1882	S 42,9683	4,6698	Soil on scree	Conglomerate	2010/12	0	0,0	0	0,0	0	0	-	Unlikely	0,00	4,32*10 ⁵
Curavacas	FC	2143	S 42,9729	4,6711	Soil on scree	Conglomerate	2010/12	32	9,0	0	0,0	0	6	0 to 0,5	Unlikely	0,00	4,32*10 ⁵
Curavacas	FC	2346	S 42,9756	4,6723	Soil over bedrock	Conglomerate	2010/12	125	35,1	14	3,9	77	4	-2,5 to 0	Yes	0,55	4,32*10 ⁵
Curavacas (2)	FC	2272	N 42,9759	4,6786	Active scree	Conglomerate	2010/12	229	64,3	0	0,0	0	2	0 to 0,5	Unlikely	0,00	4,32*10 ⁵
Curavacas (1)	FC	2277	N 42,9756	4,6786	Active scree	Conglomerate	2010/12	233	65,4	0	0,0	0	4	0	Likely	0,00	4,32*10 ⁵
Llambrión	PE	2535	N 43,1736	4,8528	Till in rock bar	Limestone	2005/07	217	60,9	0	0,0	85	15	-0,5 to 0	Likely	0,42	2,05*10 ⁵
Trasllambrión	PE	2490	N 43,1748	4,8541	Till in rock bar	Limestone	2005/07	234	65,7	2	0,6	219	8	-1,5 to -0,3	Yes	0,62	2,05*10 ⁵
Trasllambrión	PE	2360	N 43,1792	4,8533	Top debris cone	Limestone	2005/07	238	66,8	0	0,0	59	3	-0,5 to 0	Likely	0,37	2,05*10 ⁵
Jou Negro	PE	2205	N 43,2027	4,8499	Debris slope	Limestone	2005/07	121	34,0	2	0,6	113	10	-1,5 to -0,5	Yes	0,47	2,05*10 ⁵
Jou Negro	PE	2155	N 43,2022	4,8521	Till in moraine	Limestone	2005/07	238	66,8	65	18,2	235	18	-1,1 to -0,1	Yes	0,64	2,05*10 ⁵
Jou Negro	PE	2190	N 43,2019	4,8525	Till -patterned ground	Limestone	2005/07	176	49,4	63	17,7	461	40	-8,5 to 0	Yes	0,77	1,64*10 ⁵
Jou Negro (Ta)	PE	2190	N 43,2019	4,8525	Till -patterned ground	Limestone	2005/07	277	77,8	1	0,3	138	36	-2,5 to -0,1	Yes	0,37	1,64*10 ⁵
Peña Vieja	PE	2510	W 43,1747	4,8106	Debris slope	Limestone	2003/04	146	41,0	17	4,8	96	9	-1 to 0	Likely	0,41	1,64*10 ⁵
Peña Vieja	PE	2325	W 43,1753	4,8122	Small sinkhole	Limestone	2003/05	230	64,6	0	0,0	20	15	-0,2 to 0,2	Likely	0,26	2,05*10 ⁵
Lloroza	PE	1865	S 43,1597	4,8120	Moraine	Limestone	2005/07	79	22,2	2	0,6	55	8	-0,7 to 0,5	Likely	0,33	1,64*10 ⁵
Áliva	PE	1735	E 43,1944	4,7714	Soil with debris	Shales	2005/07	34	9,5	0	0,0	3	6	0 to 0,5	Likely	0,15	1,44*10 ⁵
Fuente Dé	PE	1115	S 43,1492	4,8098	Debris cone	Limestone	2005/07	0	0,0	0	0,0	0	0	-	Unlikely	0,00	2,05*10 ⁵

^[1] Washburn (1979): $h(m) = \sqrt{\frac{2 * K * FI}{C_L}} + d$; K (Conductivity J* °day); CL (Latent Heat 3,34*108J *m-3); FI (Freeze Index °day); d (depth of the register 0,1)

Table 2. Monthly distribution of F/Tc in PE and FC.
[Click here to download high resolution image](#)

Picos de Europa	Alt.	Jan	Feb	Mar	Apr	May	Jun	Jul	Aug	Sept	Oct	Nov	Dec	Total	Year
Llambrión	2.535							1		1	2	2	9	15	2006
Peña Vieja	2.510					5						3	1	9	10/2003- 10/2004
Jou Traslambrión	2.490							1			1	6		8	2006
Jou Traslambrión	2.360							1	2					3	2006
Peña Vieja	2.325	13	1					1						15	2004
Jou Negro	2.205					5						3	2	10	2006
Jou Negro (Superficie)	2.190							1	2	5	8	14	4	34	11/2005-11/2006
Jou Negro	2.190	4							4	4	10	14	4	40	11/2005-11/2006
Jou Negro	2.155				4	4						6	4	18	2006
Lloroza	1.865			7									1	8	2006
Áliva	1.720	1	1	3	1									6	2005
Fuente Dé	1.115													0	2006
SubTotal		18	2	10	5	14	0	5	8	10	21	48	25		
Fuentes Carrionas	Alt.	Jan	Feb	Mar	Apr	May	Jun	Jul	Aug	Sept	Oct	Nov	Dec	Total	Year
Espiguete	1.889						1							1	2009/10
Espiguete	2.016				1						4	4		9	2010/11
Lomas E	1.918	1	1	1									1	4	2010/11
Lomas E	2.169				9	3						5	1	18	2010/11
Lomas E	2.412						1				1			2	2010/11
Lomas W	2.163	7	1	1									9	18	2010/11
Lomas W	2.417	9	13	8								3	11	44	2010/11
Lomas N	2.415					1					1	3		5	2010/11
Curavacas S	1.882													0	2010/11
Curavacas S	2.143		2	1										3	2010/11
Curavacas S	2.346				1								4	5	2010/11
Curavacas N low	2.272						1				1			2	2010/11
Curavacas N high	2.277						1				1			2	2010/11
Subtotal		17	17	11	11	4	4	0	0	0	8	15	26		
TOTAL		35	19	21	16	18	4	5	8	10	29	63	51		

Figure 1. Location of Cantabrian Range and the massifs studied.
[Click here to download high resolution image](#)

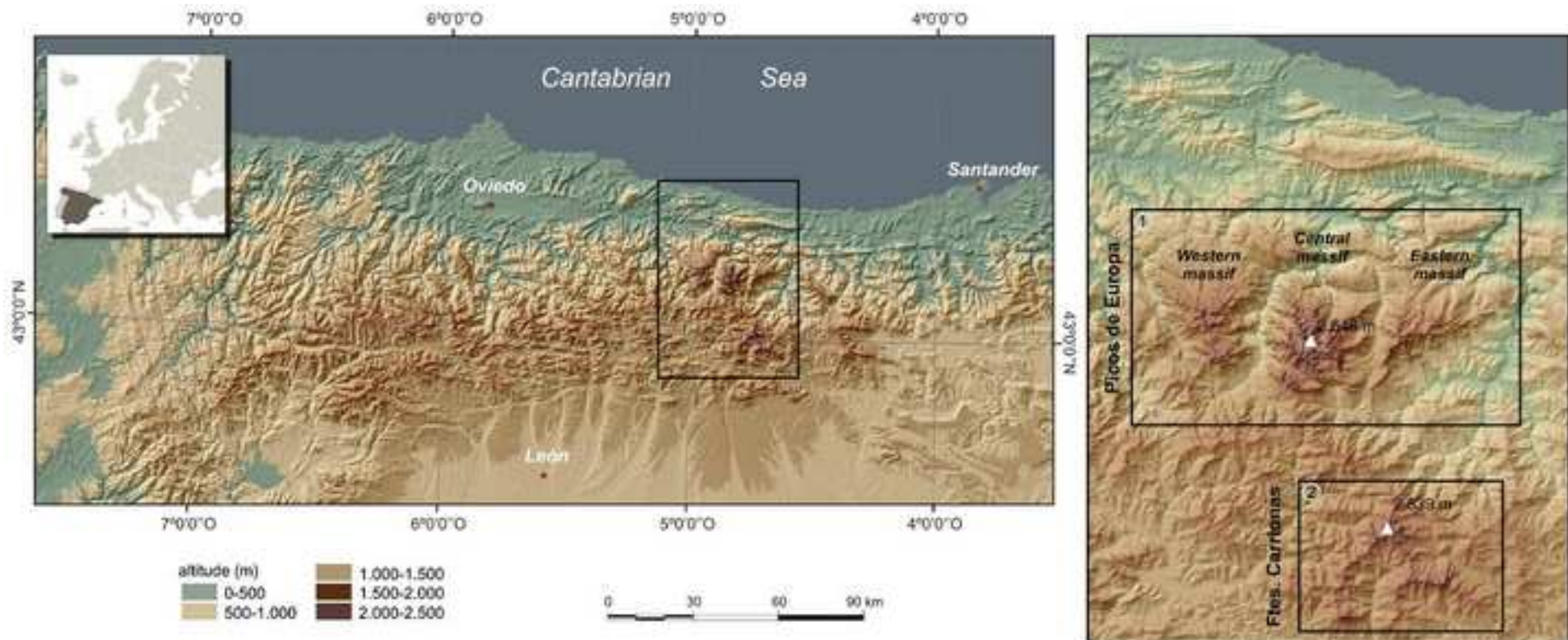


Figure 2. Locations of the thermometers in Picos de Europa massi
[Click here to download high resolution image](#)



Figure 3. Locations of the thermometers in Fuentes Carrionas ...
[Click here to download high resolution image](#)



Figure 4. Left, massif of Picos de Europa and right, massif of F
[Click here to download high resolution image](#)

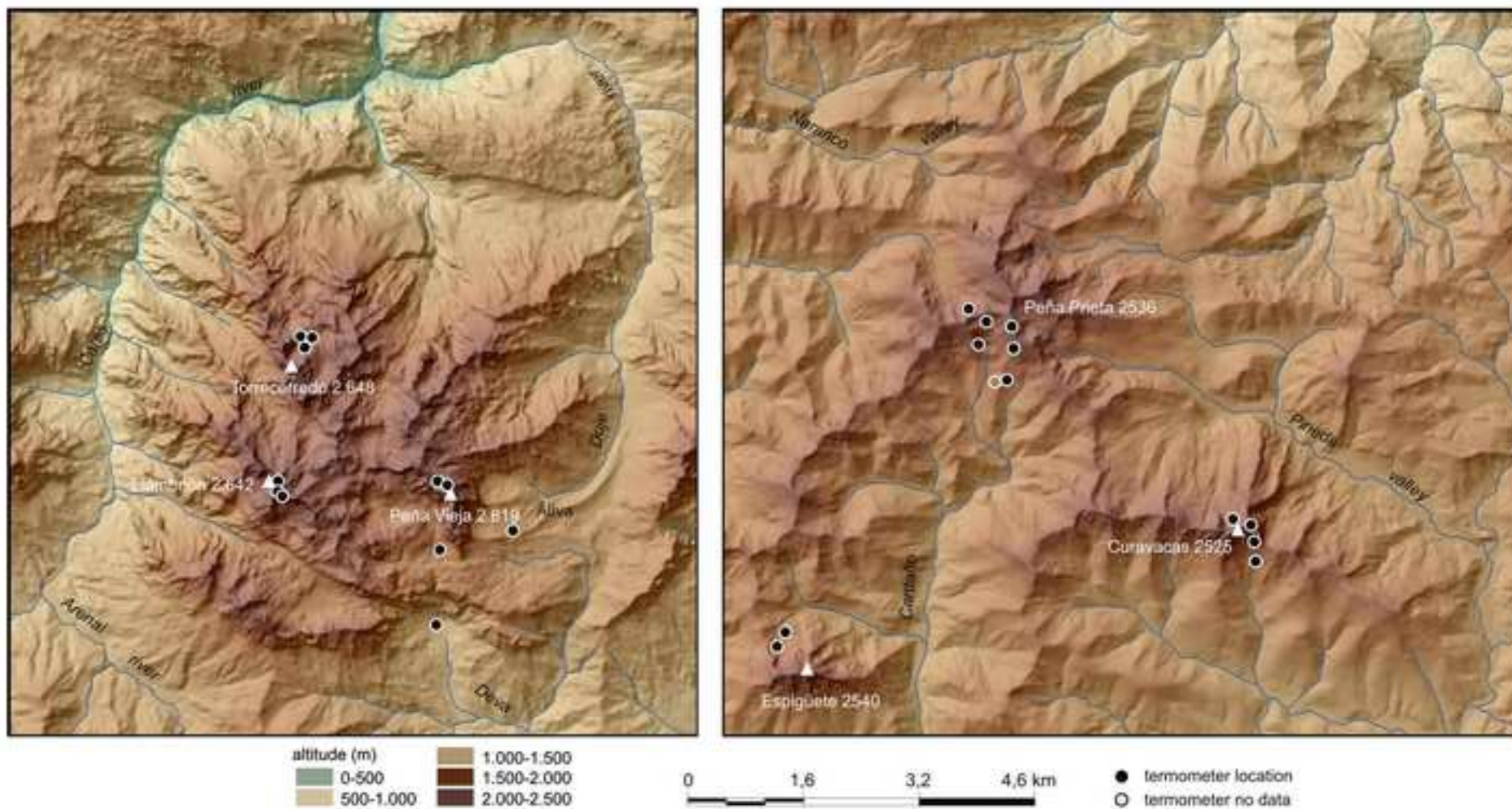


Figure 5. Air temperature and precipitation approximately in PE
[Click here to download high resolution image](#)

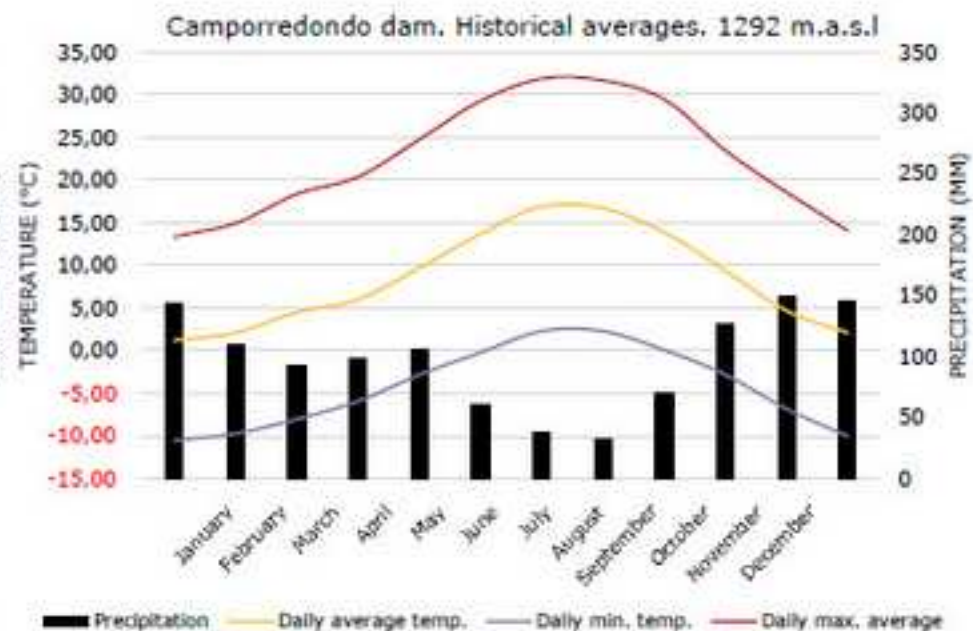
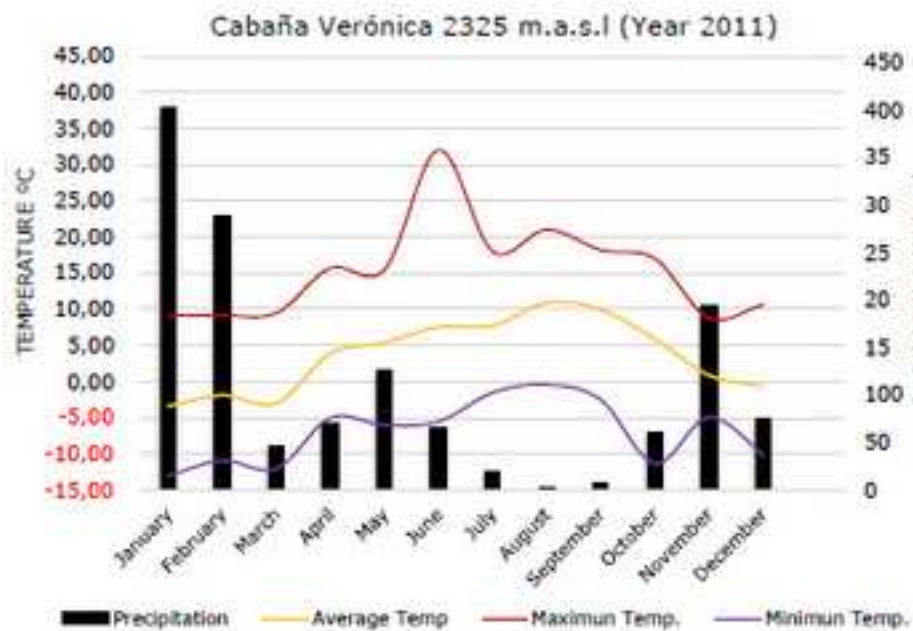


Figure 6. Correlation between thermometers in FC (triangles) and [Click here to download high resolution image](#)

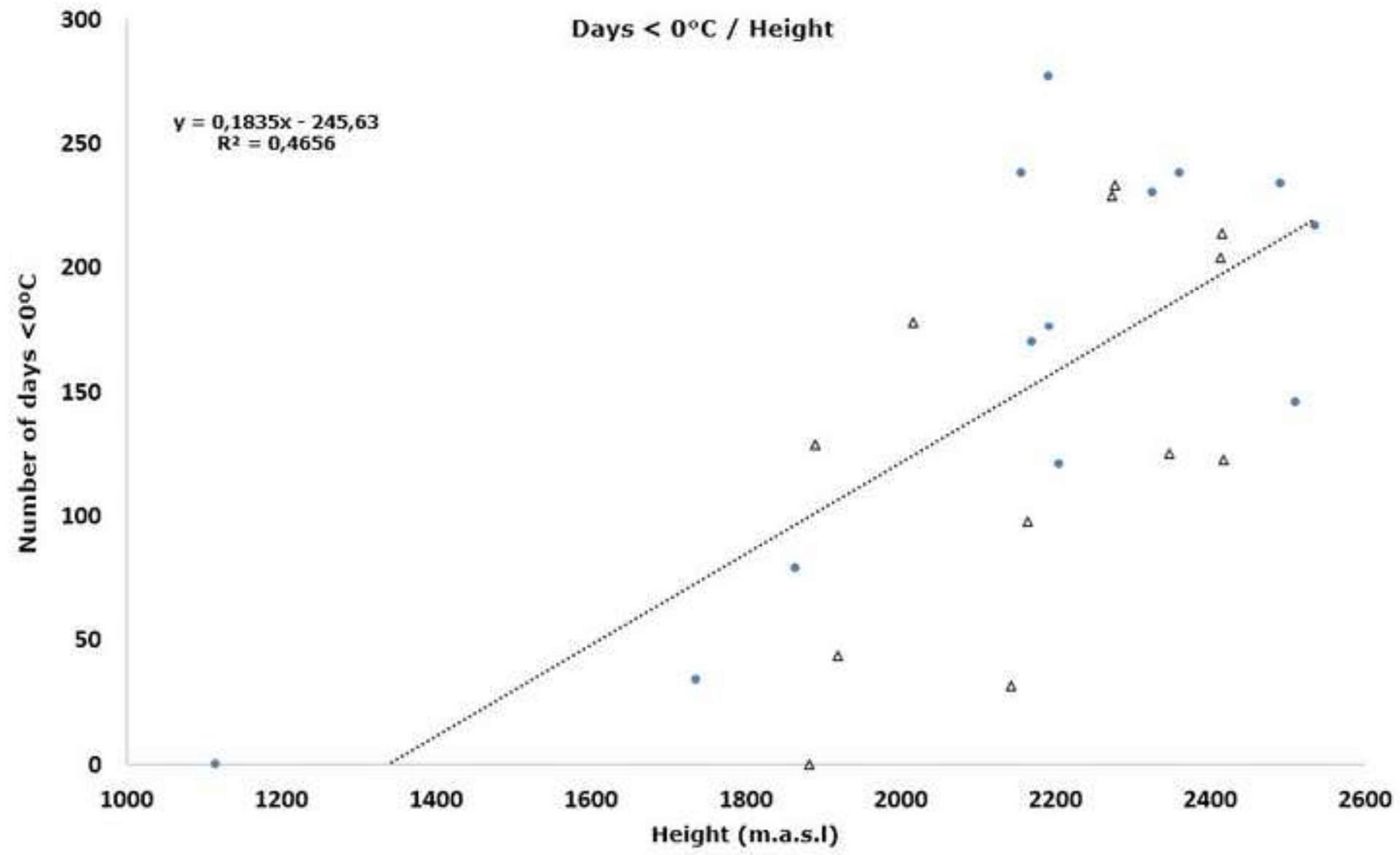


Figure 7. Ground thermal regimes of Picos de Europa

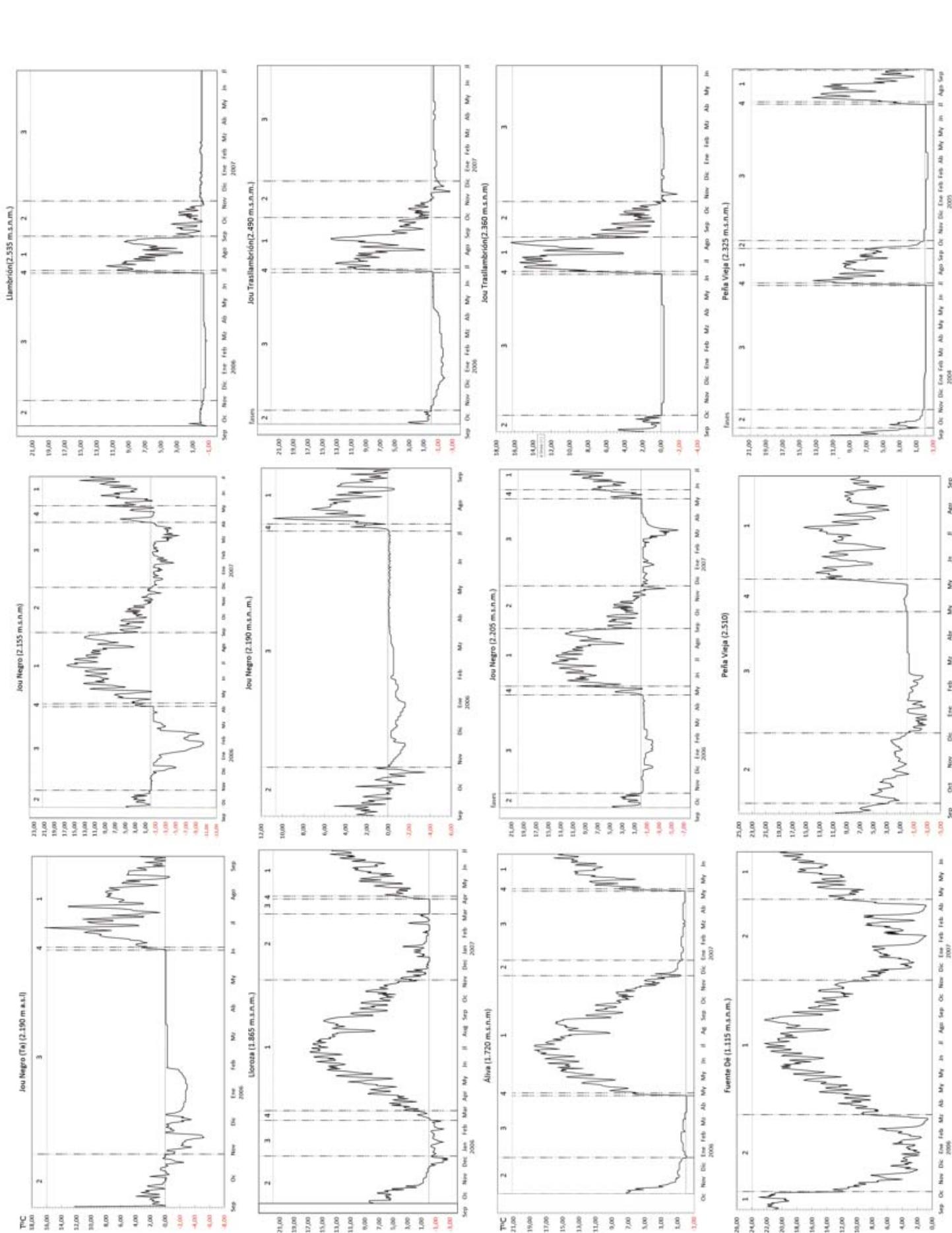


Figure 7. Ground thermal regimes of Picos de Europa

Figure 8. Ground thermal regimes of Fuentes Carrionas
[Click here to download high resolution image](#)

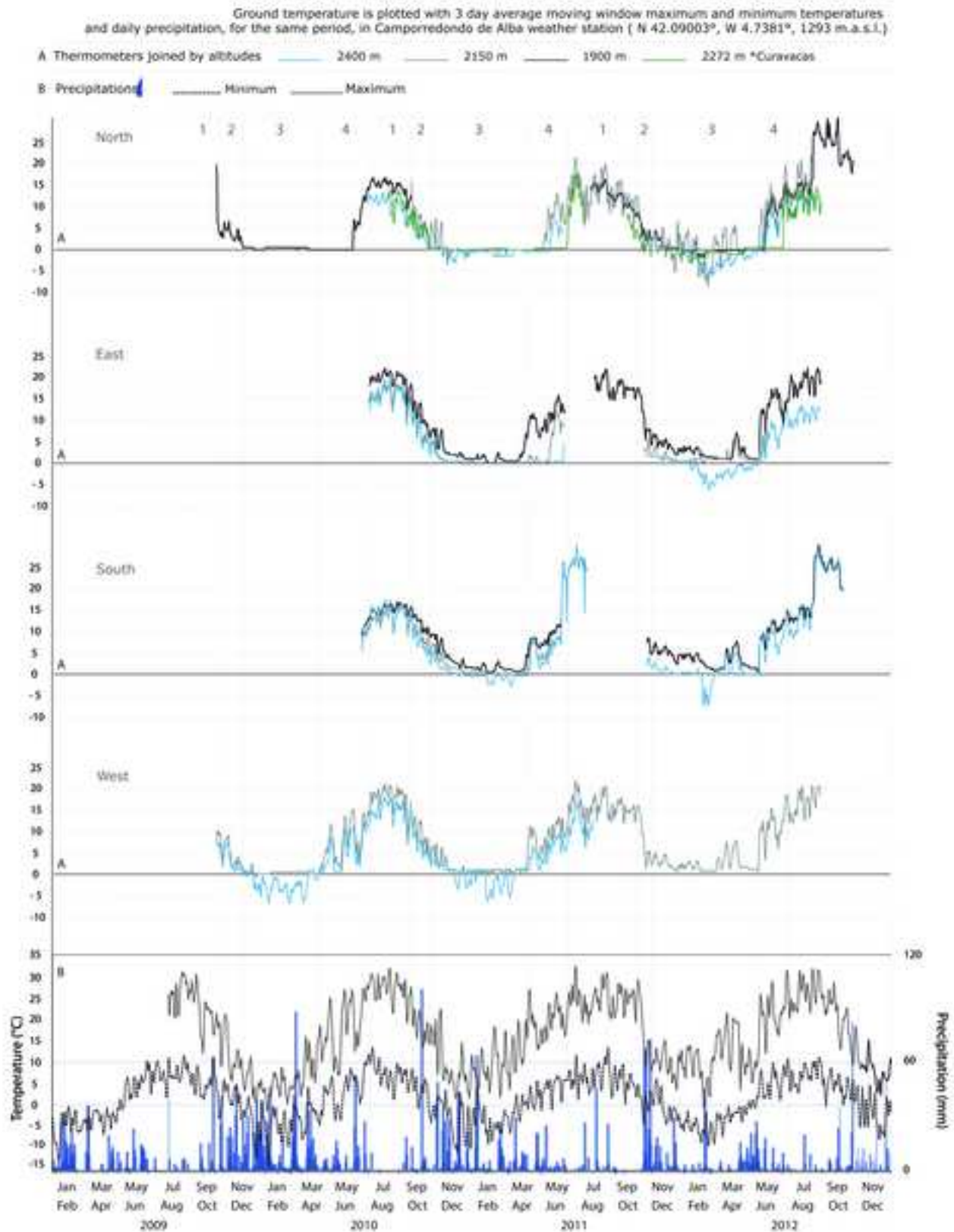


Figure 9. Environments, thermal regime, processes and active lan
[Click here to download high resolution image](#)









Environment	Geomorphic belt	Thermal regime	Processes	Active landforms	Landscape	
High Mountain	Cryonival or Upper periglacial	?	?	Crest, Summits Walls, Debris talus		
		Seasonal frozen ground Ih: 360-400 F/T: 3-14 NDTs<-2: 2-65 NDTs<0: 120-135	Cryoturbation Gelifraction Gelifluction Nivokarst Nivation Solifluction	Frost mounds Patterned ground Debris lobes Debris talus and cones Nivation hollows Prortalus rampart Nival karst		
		AAMT: <3.6°C NDTa <-2: 122 NDTa <0: 86			Possible sporadic permafrost	
		Seasonal frozen ground				
Montane	Nivoperiglacial or Lower periglacial	Seasonal frozen ground Ih: 320-360 F/T: 8-18 NDTs<-2: 2-63 NDTs<0: 80-175	Gelifraction Nivokarst Nivation Solifluction	Debris talus and cones Ploughing blocks Fines lobes Solifluction terraces Nival karst		
		AAMT: ~5°C NDTa <-2: ~45 NDTa <0: ~75				
		Not probable seasonal frozen ground Ih: 200-360 F/T: 0-8 NDTs<-2: 0-2 NDTs<0: 0-80			Nivation Solifluction Diffuse runoff Torrential	Nival karst ploughing blocks Fine lobes Solifluction terraces Debris talus Solifluction sheets
		AAMT: 5-6°C NDTa <-2: 20-40 NDTa <0: ~75				
		Not frozen ground				

Figure 10. Environments, thermal regime, processes and active la
[Click here to download high resolution image](#)




	Environment	Geomorphic belt	Thermal regime	Processes	Active landforms	Landscape
2550	High mountain (alpine)	Cryonival	Seasonal frozen ground FI: 0-379 F/T: 2-58 NDTs $\leq -2^{\circ}\text{C}$: 0-92 NDTs $\leq 0^{\circ}\text{C}$: 117-244 AAMT: 3.5°C <i>Sporadic permafrost?</i>	Gelifraction Gelifluction Debris flow Rockfall Nivation Avalanches	Blockfields Stone-banked gelifluction lobes Protalus lobe? Walls Debris talus and cones Terracetes	
2500						
2450						
2400						
2350						
2300						
2250						
2200						
2150		Nivo-periglacial	Seasonal frozen ground FI: 0-151 F/T: 6-39 NDTs $\leq -2^{\circ}\text{C}$: 0-40 NDTs $\leq 0^{\circ}\text{C}$: 0-151 AAMT: 5.2°C	Nivation Solifluction Nival abrasion Avalanches	Debris talus and cones Turf-banked solifluction lobes Terracetes Nivation hollows Nival abrasion surfaces Snow-push moraines Ploughing boulders	
2100						
2050						
2000						
1950						
1900						
1850	Mid-mountain (montane)	Infraperiglacial	Seasonal frost only on N face FI: 0-39 F/T: 0-6 NDTs $\leq -2^{\circ}\text{C}$: 0-1 NDTs $\leq 0^{\circ}\text{C}$: 0-129 AAMT: 6.3°C	Runoff Torrential erosion Solifluction (N face)	Nival terracetes Ravines	
1800						
1750						
1700						

Figure 11. A) The W face of Tres Provincias peak, where the g
[Click here to download high resolution image](#)

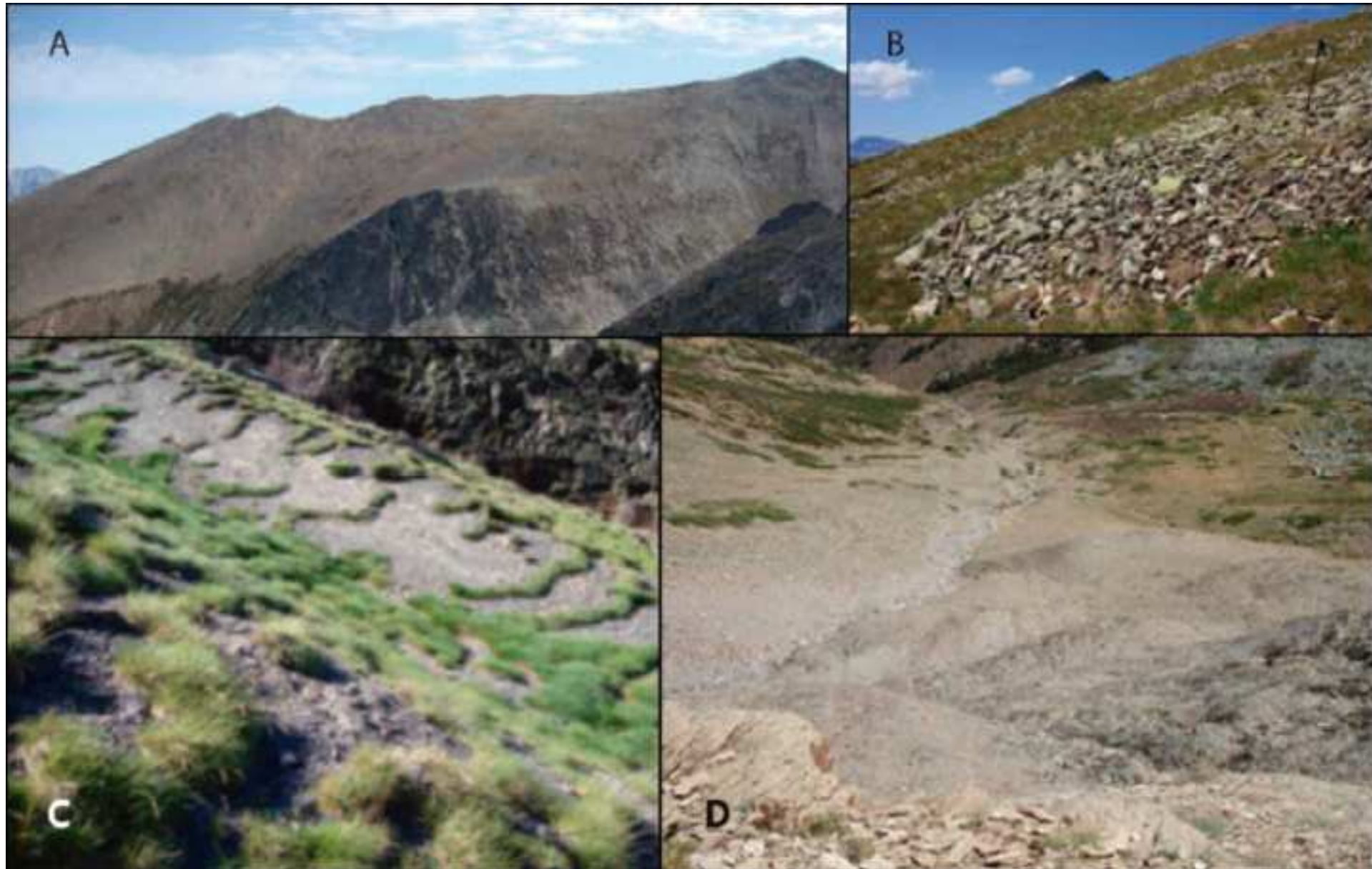
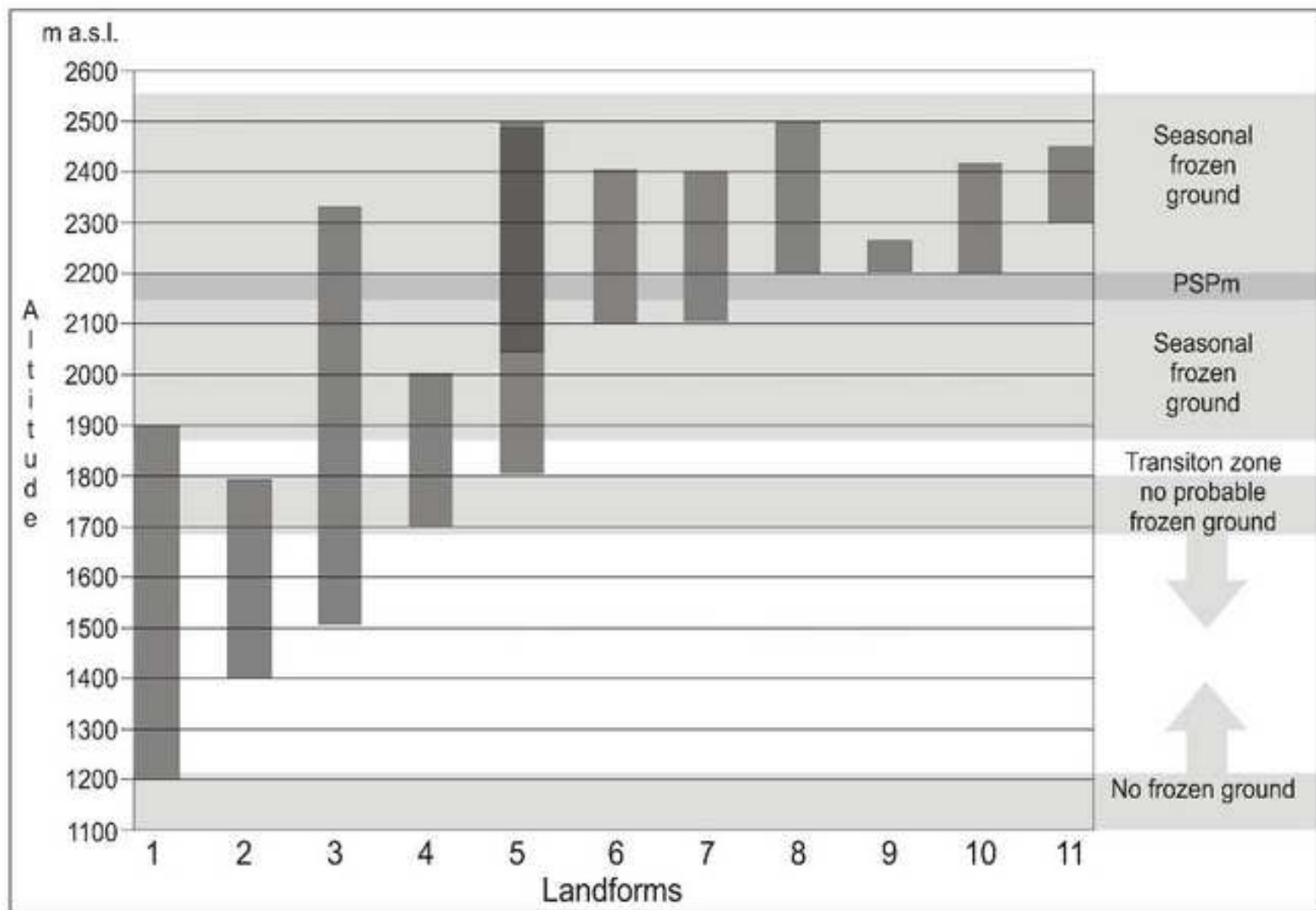


Figure 12. Altitudinal distribution of environment, ground ice, [Click here to download high resolution image](#)



PSPm, possible sporadic permafrost